
Preventing Catastrophic Camshaft Lobe Failures in Low Emission Diesel Engines

J. A. Mc Geehan and P. R. Ryason

Chevron Products Company

The appearance of the ISSN code at the bottom of this page indicates SAE's consent that copies of the paper may be made for personal or internal use of specific clients. This consent is given on the condition however, that the copier pay a \$7.00 per article copy fee through the Copyright Clearance Center, Inc. Operations Center, 222 Rosewood Drive, Danvers, MA 01923 for copying beyond that permitted by Sections 107 or 108 of the U.S. Copyright Law. This consent does not extend to other kinds of copying such as copying for general distribution, for advertising or promotional purposes, for creating new collective works, or for resale.

SAE routinely stocks printed papers for a period of three years following date of publication. Direct your orders to SAE Customer Sales and Satisfaction Department.

Quantity reprint rates can be obtained from the Customer Sales and Satisfaction Department.

To request permission to reprint a technical paper or permission to use copyright SAE publications in other works, contact the SAE Publications Group.



GLOBAL MOBILITY DATABASE

All SAE papers, standards, and selected books are abstracted and indexed in the SAE Global Mobility Database.

No part of this publication may be reproduced in any form, in an electronic retrieval system or otherwise, without the prior written permission of the publisher.

ISSN0148-7191

Copyright ©2000 CEC and SAE International.

Positions and opinions advanced in this paper are those of the author(s) and not necessarily those of SAE. The author is solely responsible for the content of the paper. A process is available by which discussions will be printed with the paper if it is published in SAE Transactions. For permission to publish this paper in full or in part, contact the SAE Publications Group.

Persons wishing to submit papers to be considered for presentation or publication through SAE should send the manuscript or a 300 word abstract of a proposed manuscript to: Secretary, Engineering Meetings Board, SAE.

Printed in U.S.A.

Preventing Catastrophic Camshaft Lobe Failures in Low Emission Diesel Engines

J. A. Mc Geehan and P. R. Ryason

Chevron Products Co.

Copyright © 2000 Society of Automotive Engineers, Inc.

ABSTRACT

With the drive to reduce emissions and improve fuel economy, fuel injection pressures have increased. This has increased Hertzian stresses on the roller follower cam system to the point that cam lobe contact fatigue failure has become the "Achilles heel" of diesel engine durability in the 1990s. Contact fatigue failures have occurred on both injector lobes and the exhaust and inlet lobes. This is particularly the case in fleets with frequent engine shut downs and starts, stop-go service and in some line-haul fleets.

This paper describes field service cam failures across several engine types and applications. In our experience supporting fleet customers in cam failure analysis, we found that a combination of ten critical independent variables must be correct in order to prevent cam lobe contact fatigue failures. These variables are each discussed separately.

In bench tests simulating stop-go applications, we found that the silicon nitride roller on a steel pin had low and constant friction under flooded and starved lubrication conditions. In contrast, the bronze pin and steel roller had severe stick-slip with very high friction, which could cause roller skidding on the cam. The silicon nitride roller and steel pin have provided long cam life in many applications.

INTRODUCTION

On-highway diesel engine emission reductions have been mandated by the U.S. Environmental Protection Agency (EPA). As a result, a 70% reduction in NO_x emissions and a 90% reduction in particulate emissions have been achieved since the 1980s by combustion process improvements and electronic fuel systems. SO_x emissions have also been lowered by reductions in fuel sulfur [1].

To help meet the emissions standards, new injection systems have been employed. In engines with displacements greater than 10 liters, the Unit Injector is most commonly used. Additionally, new fuel systems such as the Electronic Unit Pump and the Hydraulically actuated Electronically controlled Unit Injector (HEUI) have been brought into service. All employ roller follower cam systems to lower friction and increase fuel economy [2].

These changes have resulted in increased fuel injection pressures. In turn, Hertzian stresses in the roller follower cam mechanisms have increased to the point that cam lobe contact fatigue failures have become the "Achilles heel" of engine durability in the 1990s. Failures have resulted directly from increased camshaft Hertzian stresses, and also from failure to control and define a number of other critical independent variables.

Contact fatigue failures have occurred on the injector lobe and on both the exhaust valve and the inlet valve lobes. Such failures may occur independently on different lobes, or may be initiated by debris from a failed injector lobe. Camshaft lobe failures are particularly prevalent in fleets with stop-go service, or in engines operating with frequent accelerations and decelerations, such as mail delivery vehicles, garbage trucks, front loaders, and some line-haul fleets. Failures in engines in line-haul service are primarily a consequence of camshaft metallurgy, surface finish or other mechanical details, and the lack of prompt and adequate lubrication. As will become evident in the discussion, this distinction is not a rigid categorization but provides a useful starting point.

During accelerations and decelerations, skidding of the roller on the cam may occur. Skidding of the roller on the cam results when the traction force between the cam and roller is smaller than that required by the combined roller-pin friction torque and the roller inertial torque [3]. Skidding of the roller on the cam is equivalent to sliding, rather than rolling contact of the roller-cam interface, and may initiate surface contact fatigue failures.

Although a number of papers were published in the mid-1990s on cam-roller reliability and skidding, they emphasized computer simulations combined with bench testing to support improvements in cam design [3-6]. The present paper describes field service cam failures across several engine types and applications, and supplements previous work with examples of failures and analyses of failure mechanisms.

In our experience supporting customers by analysis of engine failures, a combination of critical factors must be correct in order to achieve long camshaft life under the wide range of dynamic conditions characteristic of field operation of diesel engines. These critical factors are listed below:

1. Prompt and Adequate Lubrication to Central Roller Pin and Cam-Roller Surfaces
2. Use of Oil Formulations Meeting API CG-4 or CH-4 Requirements
3. Staying Within the Stress Capability of the Cam and Roller
4. Low Friction Between the Roller Pin and Roller
5. Surface Finishes That Minimize Asperity Contact
6. Extremely Hard Cam Lobe and Roller Surfaces
7. Residual Surface Compressive Stresses
8. Flat Cam Lobe Surface and Crown Roller Geometry
9. Proper Injector and Valve Clearance to Minimize Stress, and
10. Correct Alignment of Cam Lobe and Roller

These factors are discussed separately in this paper. Examples of camshaft failure modes for a number of different engines and applications are provided. The paper is organized with brief reviews of emission standards and failure cycles, followed by reviews of the critical factors listed above. Three kinds of valve trains are considered:

- Steel Roller Follower With Needle Bearing,
- Steel Roller With Bronze Roller Pin, and
- Ceramic Roller With Steel Roller Pin

COMPLYING WITH EMISSIONS REGULATIONS HAS RESULTED IN INCREASED INJECTION PRESSURES AND CAM HERTZIAN STRESS

U.S. EPA standards control diesel particulate and NO_x emissions, and both have been reduced stepwise. (See Figure 1.) Since October 1998, these emissions have

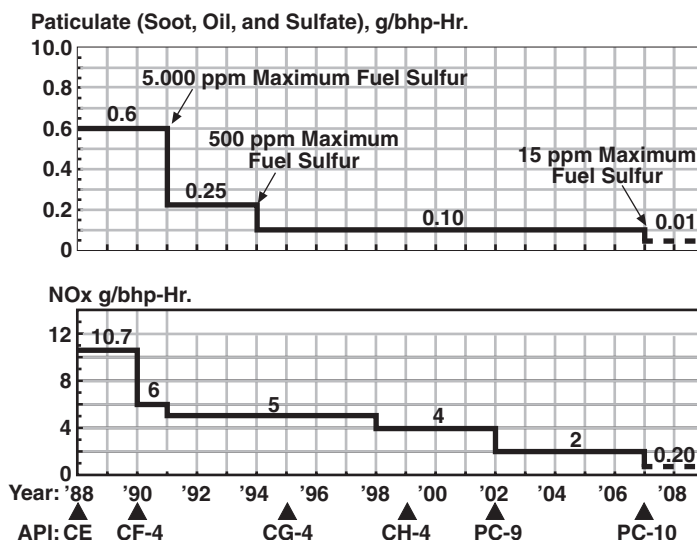


Figure 1 – EPA’s reductions in particulate, NO_x and fuel sulfur level for diesel engines. Paradigm shifts in oil quality levels driven by exhaust emission regulations.

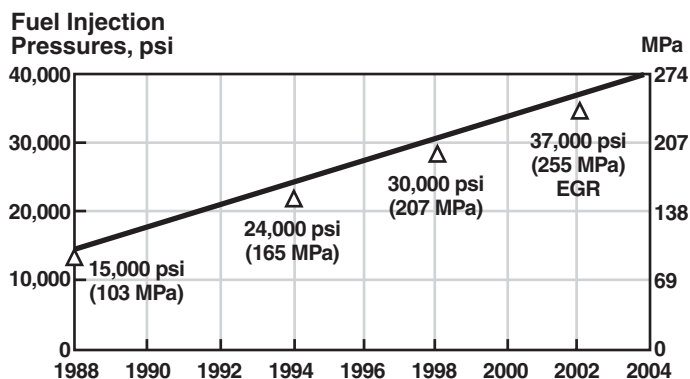


Figure 2 – Trend to high fuel injection pressures with unit injectors with reduced emissions.

been determined by both the Federal Test Procedure for urban areas and by the 13 mode European steady state cycle for rural and on-highway operations.

Reducing peak combustion temperatures is the approach taken to control NO_x. Retarded fuel injection timing lowers peak combustion flame temperatures and reduces NO_x formation by displacing the combustion event until later in the expansion stroke. This utilizes the mechanical expansion of combustion volume to offset increases in pressure and temperature.

Several factors affect particulate control. They include: fuel sulfur concentration, air-fuel ratio, in-cylinder air swirl, piston crevice volume, injection quality, and fuel injection pressure. Better atomization of fuel is required, including spray shape, a “soft” beginning and a “sharp” end of injection [7].

Control of both NO_x and particulates has resulted in significant increases in injection pressures with unit injectors. It is expected to increase still more by 2002 with the application of Cooled Exhaust Gas Recirculation (EGR). Cooled EGR adds an inert gas to the charge, reducing flame temperatures and maintaining fuel economy while meeting the 2 g/bhp-hr NO_x requirement. (See Figure 2.)

In 2007, the proposed emission levels are to be tenfold lower than 2002. Particulate is proposed to be 0.01 g/bhp-hr, with NO_x at 0.20 g/bhp-hr! To achieve these standards we expect the use of cool EGR, NO_x adsorber catalysts, and particulate traps. In addition, it is proposed to lower fuel sulfur levels to 15 ppm maximum for catalysts compatibility and to reduce particulate.

FAILURE CYCLES

Since 1988 when diesel emissions were first regulated, the increase in injection pressures has increased cam Hertzian stress in some cases to 250,000-300,000 psi (1,722-2,067MPa) and above. Correspondingly, cam failures appeared in the early 1990s because detailed improvement in cam quality and prompt lubrication were not applied.

Cam failures have occurred in line-haul fleets if certain important factors are not correct. They have been most prevalent in fleets operating in stop-go cycles, typically, mail fleets, garbage trucks, and pick-up and delivery service. In addition, off-highway vehicles such as front loaders that meet on-highway emissions standards have had cam failures.

The Electronic Control Module (ECM) has permitted the fleet owner to increase fuel economy by minimizing idling time. With the ECM, idling may be limited to 3 minutes. To quote a customer, "These trucks do not idle." This limitation may result in repeated starting and stopping of the engine, with frequent accelerations and decelerations. In addition, at night when the truck is parked, the ECM can be set to maintain cab heating by starting and stopping the engine to maintain coolant temperature. This results in the engine starting and stopping all night!

Rapid changes in engine speed may result in roller skidding on the cam lobe. Accelerations are likely during start-up. Also, during the time the engine is off, oil may drain away from the critical cam-roller and roller pin-roller interfaces. Thus, prompt and adequate lubrication is critical at startup. Not only are the roller surfaces in relative sliding motion, but enough oil may have drained away that the remaining oil film is too thin to separate the roller contacts sufficiently. Increased friction during this critical moment is evident in the wear analysis, as discussed below.

Dynamometer testing to simulate the problem involves frequent cycles from low idle to high speed, peak torque, and peak power. Elimination of the dynamometer can

produce very fast accelerations and decelerations with significant roller on cam lobe skidding.

PROMPT AND ADEQUATE LUBRICATION

In valve trains operating at high Hertzian stresses, it is important to provide prompt and adequate lubrication at both the roller-pin and the needle bearing and roller-cam lobe interfaces, particularly on cold startup and on accelerations of stop-go vehicles at normal operating temperatures. This is best achieved in the V-8 configurations with a central cam using hydraulic lifters. Oil is thrown off the crankshaft and, additionally, flows from the hydraulic lifters each time the camshaft lifts the valves. (See Figure 3.) In this case, the cam system is quickly flooded. Also, the Electronic Unit Pump system, with the camshaft located low in the block beside the crankshaft, provides rapid lubrication of cam and rollers. However, as the camshaft location is moved higher in the block, particularly with overhead cam systems, lubrication times can be longer.

Cold Temperature Pumping Times in Cummins M-11 Celect

To determine oil pumping times to critical components, we conducted low temperature oil pumpability testing using a Cummins M-11 Celect engine with oil pressure sensors on the oil gallery, turbocharger bearing, rocker shaft bearing, and roller pin. (See Figure 4.)

The engine test stand configuration had a:

- Maximum Low Temperature of -30°C
- Motoring Dynamometer Drive Capacity of 300 bhp
- Starter Mounted on a Dynamometer Powered by a 12-Volt Battery
- Computer System With the Following Data Acquisition Capabilities:
 - 0-60 Seconds: 10 Observations Per Second
 - 60-300 Seconds: 5 Observations Per Second

The steps in the evaluation process were as follows:

- Flush the Engine
- Motor Engine to Sump Temperature of 80°C, to Simulate Hot Shut Down
- Set the Test Cell at Target Temperature and Cool for 16 Hours
- Bring to 200 rpm Using the Starter Motor for 5 Seconds
- Increase Engine Speed to 1200 rpm
- Run the Engine for 5 Minutes

The procedure of using a starter motor for 5 seconds and then moving to the dynamometer at 1200 rpm was to simulate a starting condition in the field.

All the engine tests were conducted at -15°C (5°F). This was the cold cranking limit for SAE 15W-40 oils, as defined by SAE J300 at the time the engine test program was conducted. First, we evaluated four commercial API CG-4/SJ--SAE 15W-40 oils.

The full study in this program is reported in the paper "Low Temperature Pumpability in Emission Controlled Diesel Engines" [8]. We will report only the times to pressurize the roller pin and the rocker shaft in this paper. The rocker shaft is reported as it relates to overhead camshaft lubrication times.

In evaluating three commercial API CG-4/SJ –SAE 15W-40 oils, the times to lubricate the roller follower gallery did not start until 20-30 seconds after engine start and did not reach full pressure for 50 seconds! (See Figure 5.) The time to lubricate the rocker shaft varied from 75-95 seconds, which related to the oil's viscosity, as measured by the Mini-Rotary Viscometer TP-1 (MRV TP-1) at -25°C . The lower the viscosity the quicker the pumping times. (See Figure 6.) All the oils met the SAE J300 specifications for SAE 15W-40 oils.

In a second study we investigated the effect of viscosity grade on oil pumping times, using API CG-4/SJ oils. The SAE 5W-40 Synthetic had quicker pumping times than the SAE 10W-30 and 15W-40. This was particularly evident in the time to lubricate the rocker shaft. Times ranged from 35 to 75 seconds. (See Figures 7 and 8.)

The above tests were conducted with fresh oils at -15°C , and indicate the delay times to lubricate critical components, such as the roller pin and overhead camshafts [8].

Adequate lubrication is critical, especially in applications of stop-go engines where the oil could quickly drain from the cam system, particularly the roller pin. The optimum clearance between the pin and roller will affect the drainage of oil and its retention. Finally, the volume of oil reaching the cam system is important to insure that these components are fully flooded during operations. These volumes may be 8-12 gallons/min. (30-45 L/min.) in 12-liter overhead cam engines with no field failures.

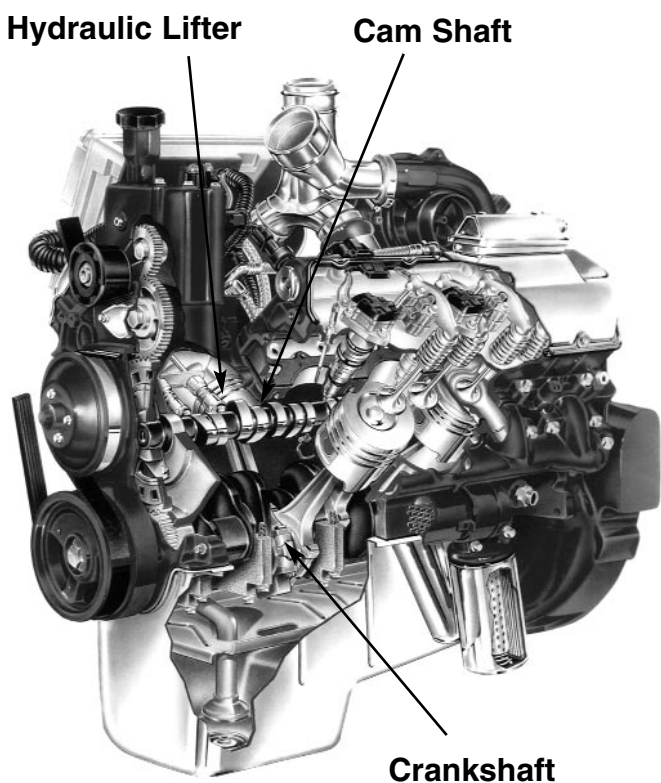


Figure 3 – V-8 configuration provides fast and adequate lubrication. Oil thrown from both crankshaft and down from hydraulic lifters on to cam lobes.

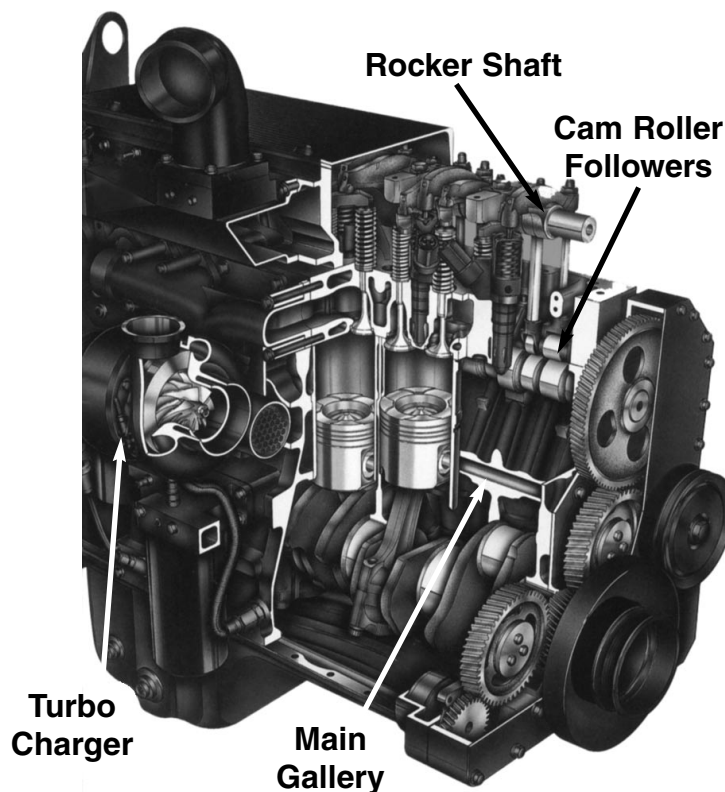


Figure 4 – Cummins M-11 low temperature pumpability test illustrating position of pressure transducers in: main oil gallery, turbocharger cam-roller follower gallery and rocker shaft.

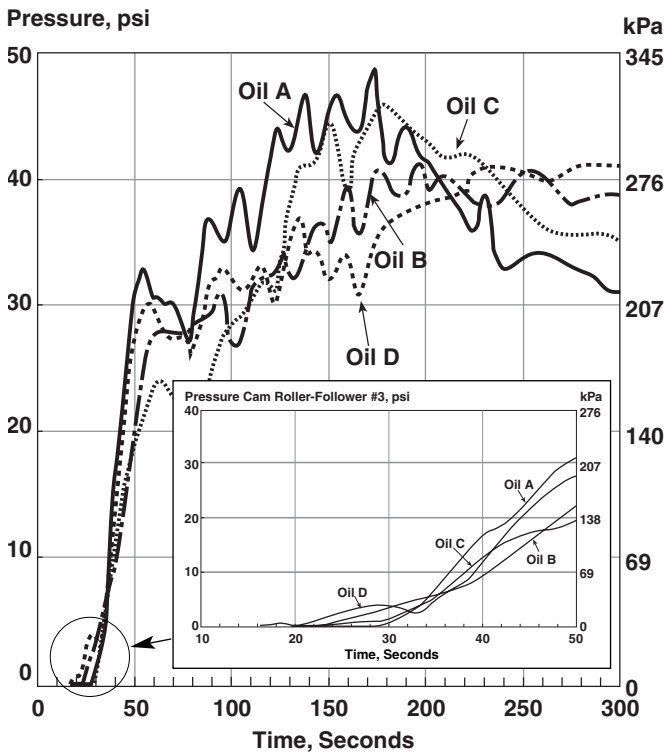


Figure 5 – Cummins M-11 low temperature pumpability at -15°C. Pressure at roller follower #3. Comparison of four commercial API CG-4/SJ – SAE 15W-40 oils.

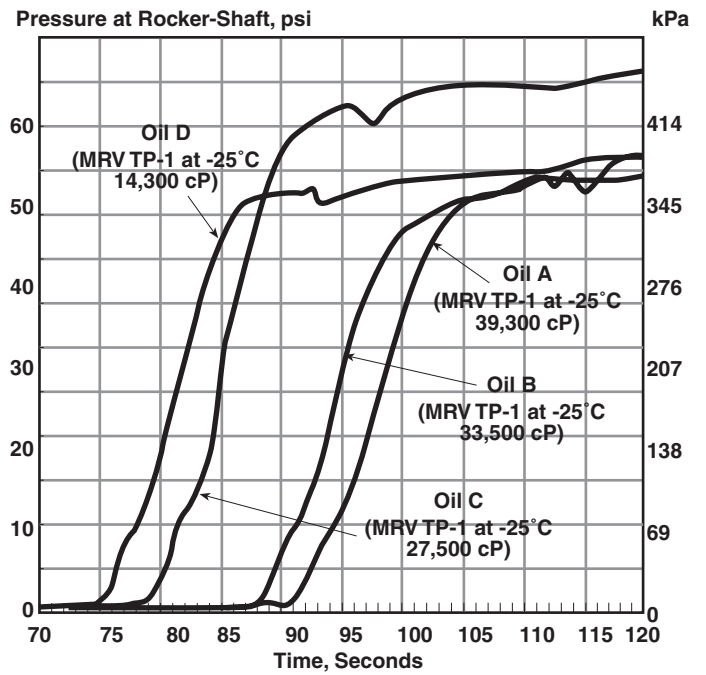


Figure 6 – Cummins M-11 low temperature pumpability at -15°C. Pressure at rocker-shaft. Comparison of four commercial API CG-4/SJ – SAE 15W-40 oils and MRV TP-1 viscosities at -25°C.

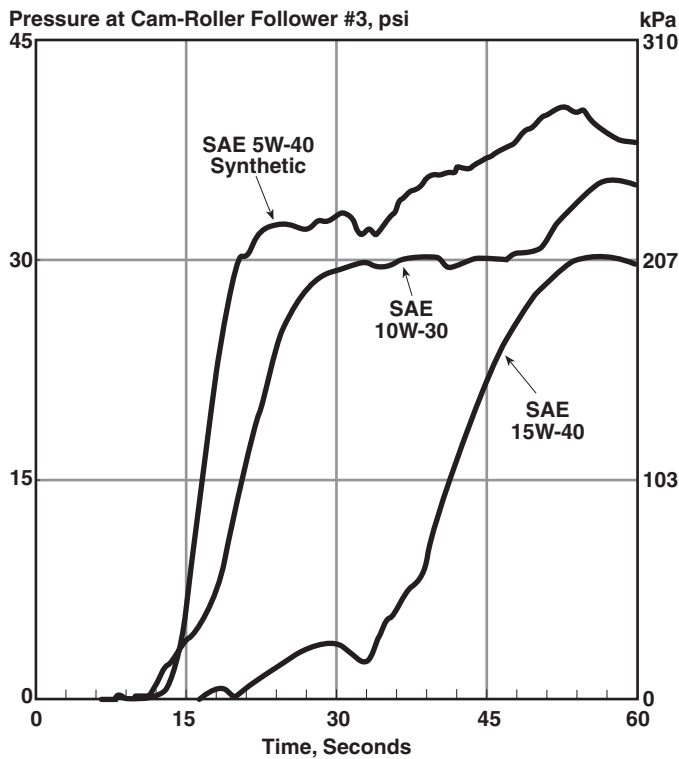


Figure 7 – Cummins M-11 low temperature pumpability at -15°C. Pressure at Roller Follower #3. Comparison of SAE 5W-40 synthetic, 10W-30 and 15W-40 grades.

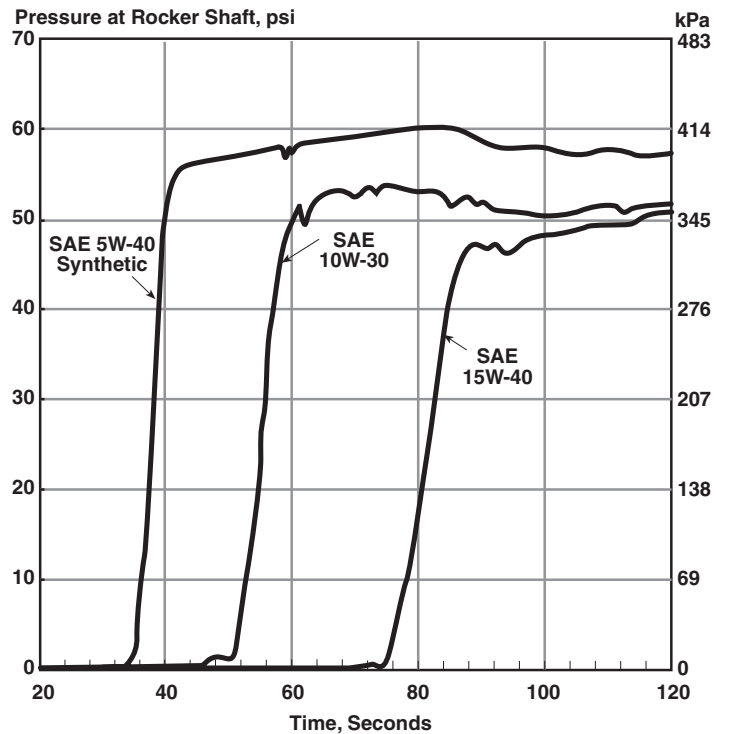


Figure 8 – Cummins M-11 low temperature pumpability at -15°C. Pressure at rocker shaft. Comparison of SAE 5W-40 synthetic, 10W-30 and 15W-40 grades.

USE OF API CG-4 AND API CH-4 OIL FORMULATIONS FOR NEEDLE BEARINGS AND STEEL ROLLERS

Prior to the 1988 emission regulations, cam failures occurred in pick-up and delivery trucks or ambulances with V-8, 6.2-7.3 liter engines. These engines had high idle times with rapid accelerations that could produce higher soot levels in the crankcase oil.

The above engines used steel roller followers with needle bearings in the hydraulic lifter. (See Figure 9.) In order to maximize load capability, the needle bearings are not in a cage, but are "free" within the roller. Without the cage the needle bearing can skid on the shaft due to lack of alignment.

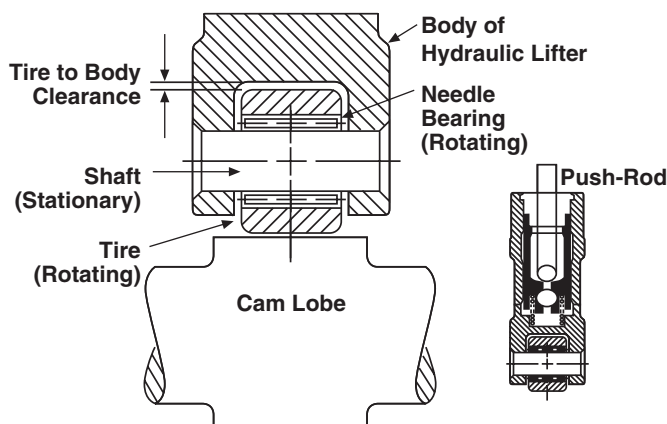


Figure 9 – GM 6.2 liter engine roller follower configuration

In field failures, polishing of the center stationary shaft, with contact fatigue at the ends where the needle radius was positioned, identified the initial failure [9]. Soot polishing could progress to catastrophic failure of the pin and the cam. Note the misalignment of needles to the center pin in the failed roller. (See Figures 10 and 11.)

The engine oils from these vehicles had 2-4% soot, yet there was no engine test in the API CF-4/SF category in which to evaluate diesel oils with soot for valve train protection. Consequently, an engine test cycle to simulate this failure mechanism was developed by GM in their 6.2-liter engine, and this resulted in 5% soot in 50 hours at 1000 rpm. Limits are set on the amount of wear on the central pin. This test was incorporated into the API CG-4 with a limit of 0.45 mils (11.4 μm) and CH-4 with a reduced limit of 0.30 mils (7.62 μm) [9-10].

This test simulated the wear problem with high and low wear in oils, as shown on the center pins. (See Figures 12 and 13.) Subsequent field testing demonstrated that oils which qualified as low wear in this test provided low wear in the field, compared to oils which failed the test and produced high wear in the field. (See Figure 14.)

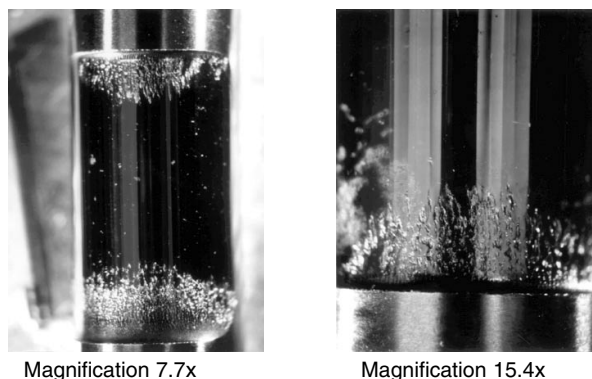


Figure 10 – GM 6.2 liter roller follower polishing and surface fatigue to the stationary shaft – field parts from ambulance fleet.

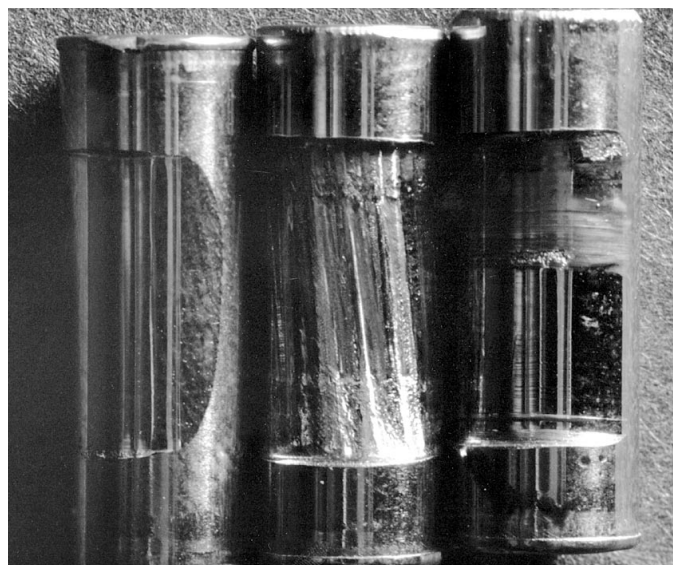


Figure 11 – 6.2 liter engine – catastrophic failure of central stationary shaft from field.

Polishing failures of this roller follower were eliminated by formulating engine oils that provided a protective wear film on the steel roller and needles in spite of 5% soot in the oil. Using low wear oils, we demonstrated that phosphorous, sulfur, and zinc from the zinc dithiophosphate (ZnDTP) had adsorbed and reacted to provide an anti-wear film. (See Figure 15.)

To insure this low wear, it is necessary to have a critical balance of additive components in the formulation, which compete for the surface, yet allow the ZnDTP to effectively adsorb and react to provide a protective film. In addition, the formulation must have adequate soot dispersancy to reduce the rate of soot abrasion of the anti-wear film.

These findings are supported by other studies. Kim et al. found that increasing the ZnDTP and the dispersant reduced wear [12]. Bardasz et al. found that low levels of wear can be maintained if the soot is well dispersed in an

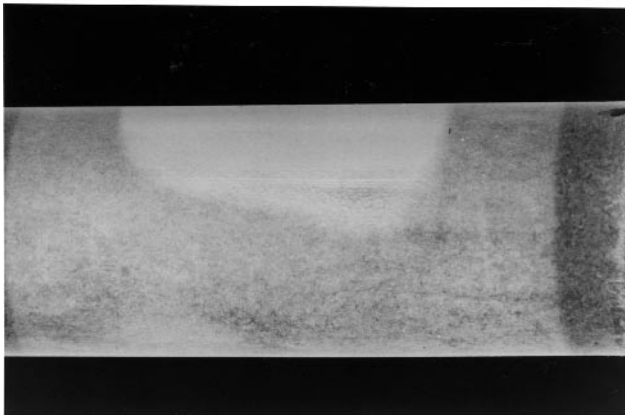
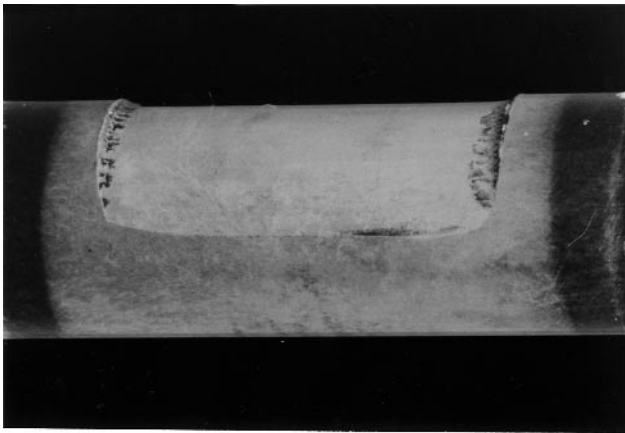


Figure 12 – Stationary shaft from GM 6.2 liter 50-hour engine dynamometer test. Top axle was double length (100 hours) test with TMC1001 (REO 217/91). Bottom axle used REO 203/83.

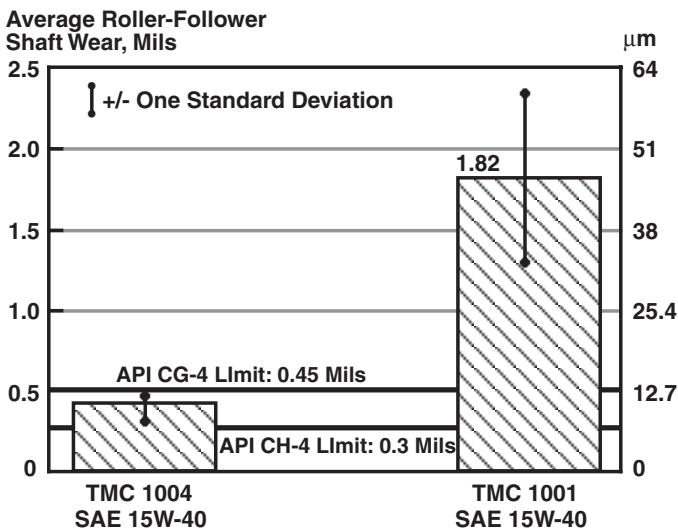
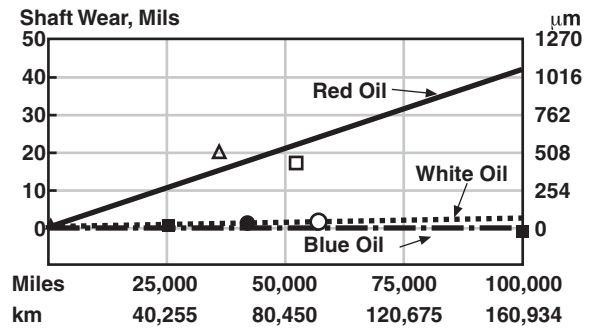


Figure 13 – GM 6.2 liter – 50-hour roller follower wear test with API CH-4 and CG-4 limits compared to low and high wear reference oils.



Oil	Red	White	Blue
Truck	△ □	● ○	■
Shaft Wear Mils	1.6	0.7	0.2
Inches	0.0016	0.0007	0.0002
µm	40.6	17.8	5.1

Figure 14 – Correlation of data between GM 6.2 liter field tests and GM 6.2 liter 50-hour dynamometer test results. Blue oil demonstrated zero wear at 100,000 miles (160,934 km) and lowest wear in 50-hour dynamometer test.

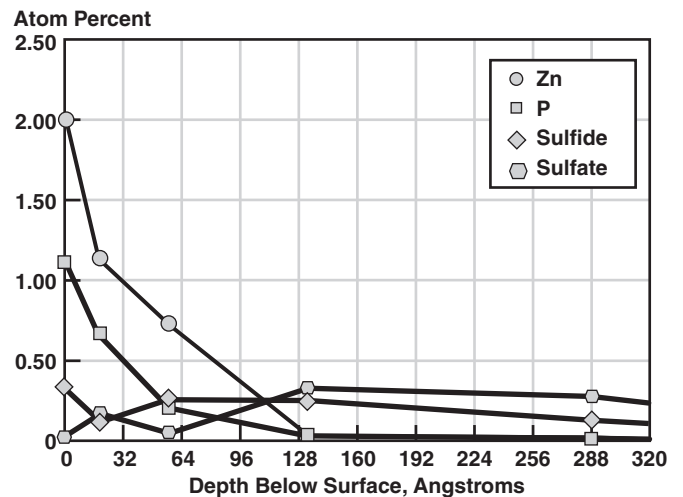


Figure 15 – Electron spectroscopy for chemical analysis (ESCA) depth profiles for low wear 6.2 liter stationary axle from 50-hour test. Phosphorous, zinc and sulfur adsorbed on low-wear axle, providing a protective wear film.

oil with adequate ZnDTP [13]. Through understanding of the formulation solutions, wear mechanisms were controlled in these engines, using both the API CG-4 and API CH-4 oils.

Subsequent testing verified that oil formulations with API CG-4/CH-4 quality oils could provide low wear with the range of sulfated ash and viscosity shown below:

- Sulfated Ash From 0.85-1.5%
- Viscosity Range: SAE 0W-30, SAE 30 to SAE 15W-40 (See Figure A-1)

Oil Film Thickness in Needle Bearings

In considering film thickness on the stationary shaft, it is important to recall that for cylindrical surface contact the oil film thickness calculation developed by Dowson and Higginson [14] involves the square root of the viscosity! See below:

CYLINDRICAL SURFACES IN CONTACT

$$h = \frac{1.6\alpha^{0.6} (\eta_0 u)^{0.7} (E)^{0.03} R^{0.43}}{w^{0.13}}$$

where:

- α = Pressure Coefficient of Viscosity
- η_0 = Viscosity at the Contact Entrance
- u = Surface Speed
- E = Young's Modulus of Elasticity (of the Rollers)
- h = Film Thickness
- R = Radius R1 and R2 Radii of Roller and Shaft
- W = Load

APPROXIMATE (DOWSON AND HIGGINSON):

$$h = 5 \times 10^{-6} (\eta_0 R)^{1/2}$$

where:

- h = Film Thickness

It is important to note that in calculating the film thickness between cylindrical surfaces in contact, the square root of the viscosity is used at its operating temperature, which can be 100-150°C! Consequently, low viscosity oils can provide wear protection if they are correctly formulated.

PREVENTING CORROSION OF THE BRONZE PIN IN STEEL ROLLER

The majority of engines in the U.S. with over 10 liters displacement use a steel roller with a bronze pin. To ensure adequate engine durability, it is necessary for a combination of critical parameters to be correct, as any one may cause a failure. (See Figure 16.)

In the early 1980s, prior to diesel engine emission regulations, bronze pin corrosion occurred which resulted in catastrophic camshaft failures [15]. This was a result of an additive -- molybdenum dithiophosphate -- being added to fully qualified API CD-SF-SAE 15W-40 oils, with the claim of fuel economy improvement. The addition of 1% of molybdenum dithiophosphate resulted in corrosive wear of both the bronze pins and the bronze wrist pin bushings. (See Figure 17.)

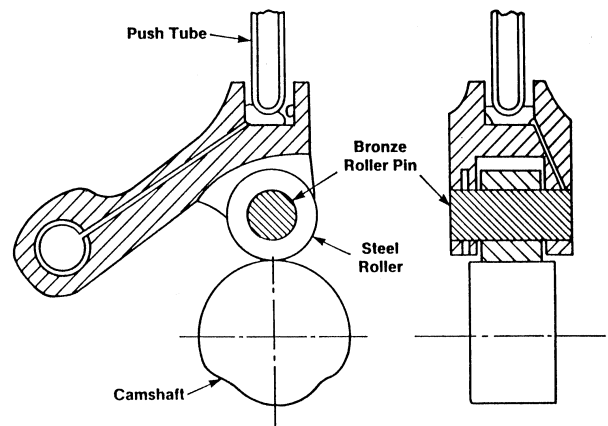


Figure 16 – Camshaft and roller follower assembly with bronze pin and steel roller.

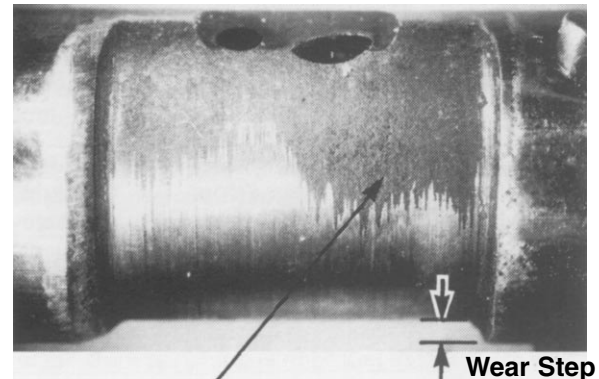


Figure 17 – Corrosion of roller follower bronze pin from the field.

X-ray powder diffraction of the deposit on the bronze pin identified $Cu_{1.8}S$, and Electron Spectroscopy for Chemical Analysis (ESCA) found over 40% cuprous sulfide. This analysis and bench test definitively identified corrosion of the pin [16]. To guard against such failures, supplementary additives should never be added to fully formulated API qualified oils, unless the full battery of sequence tests is run to confirm that no harm is caused by the modified formulation.

API CG-4/SH and CH-4/SJ oil categories now require three tests to exclude oils that might cause corrosion. They are the L-38 gasoline test for bearing corrosion of copper-lead bearings; Mack T-9 test for bearing corrosion of copper-lead bearings; and Cummins bench test, which uses strips of copper, lead, phosphor-bronze and tin immersed for 168 hours at 121°C [17].

This sequence of tests has eliminated this corrosion problem in the field. But extra components should not be added to fully qualified API products as unknown complex reactions can take place within additive systems and can cause catastrophic failures, as discussed above.

In the following discussions on rolling contact fatigue failure of the cam and roller, no bronze pin corrosion was found in any of the bronze pins from the field.

MICROFINISHING OR SUPER-FINE FINISHING OF CAM AND ROLLER TO PREVENT ASPERITY CONTACT

Improper surface finish of the cam and roller has resulted in cam-lobe failures due to contact fatigue. This section will first review some of the recent literature on this topic, followed by our own investigations and recommendations.

Literature Review

Studies by Sui and Torng indicate surface roughness to be the most influential parameter affecting cam and roller life and reliability. Decreasing surface roughness will significantly increase cam and roller life. This phenomenon is due to the fact that as the surface roughness decreases, the influence of the asperity contact pressure decreases [4].

However, Duffy [5] and Bair and Winer [6] have shown that smoother surfaces increase roller sliding. Sliding of the roller is detrimental, because in pure rolling the maximum stress in a nonconformal contact is a few microns below the surface. But if sliding occurs, the area of maximum stress moves towards the surface and may initiate contact fatigue failure, according to Hoglund [18].

In addition, Lee and Patterson [3] show that cam-roller follower lubrication involves both the elastohydrodynamic (EHD) and mixed lubrication regimes. Lubrication around the cam flank is considered to be elastohydrodynamic since the entraining velocity is very high, leading to a thick film. But the lubrication around the cam nose is considered to be mixed lubrication since the entraining velocity is low and the applied load is very high. They indicate that cam lubrication is in the boundary lubrication regime (i.e., mixed lubrication regime) from -30° to $+30^\circ$ from the cam nose. Their calculated oil film thickness in this region was 0.12 micron!

The contact surfaces are separated by a thin oil film at very high pressures. Quoting Lee and Patterson [3]: "From a comparison of the tractive force and the friction force, we can predict the roller slippage at the cam flank area and around the base circle. At the cam flank area, the slippage is caused by insufficient friction force compared to the tractive force since the roller inertia is very large in this area. Around the cam base circle, most of the friction is produced by hydrodynamic rolling friction, which gives a very low friction force. This is because the oil film thickness is greater than the surface roughness. The slippage in this area tends to increase with higher engine speed due to the increased roller pin friction."

Film Thickness Using Elastohydrodynamic (EHD) Film Thickness Measurements

In order to better understand film thickness between the cam and the roller using API CG-4/SJ SAE 15W-40 oils, we contracted Wedeven Associates to measure the EHD film thickness using Optical Interferometry over a range of temperatures [19].

These measurements are carried out on a tribometer with a transparent disk and a solid ball. The disc and ball are separately rotated, hence the slide/roll ratio can be varied. For these measurements the disc and ball were rotated at the same speed. The ball was beneath the disc, and the thickness of the oil film was measured by optical interferometry, with light passing through the disk. (See Table A-1.)

EHD film thicknesses were measured for two different API CG-4/SJ SAE 15W-40 formulations using six different base stocks. These base oil stocks included Group I and Group II, and ranged in saturate levels from 99.5 to 66%. This basically covered all hydrocracked and solvent refined base stocks used in the U.S. (See appendix for base oil details in Table A-2 & A-3.)

EHD film thicknesses were first obtained for the base oils themselves. In all cases the base oils were blended in the same ratio of base oil viscosity grades used in preparing the fully formulated oils. Secondly, the EHD film thicknesses were measured with these base oils with the additive package and V.I. improver added. The final formulations were blended to nominal 15 cSt viscosity at 100°C .

- The fully formulated oils have thicker EHD films than their base oils. This was attributed to the increase in viscosity provided by the additives, such as V.I. improvers [20]. (See Figures 18-20.)
- Within experimental error, the API Group II and Group I fully formulated API CG-4/SJ SAE 15W-40 oils have the same EHD film thickness over a temperature range of $25\text{-}100^\circ\text{C}$.
- The two different formulated API CG-4/SJ SAE 15W-40 oils have the same EHD film thickness using both Group I and Group II base stocks. (See Fig. 20)

At 100°C and a Hertzian stress of 0.59 gpa (85,6313 psi), the oil film thickness was 0.10 micron. (See Figure 18-20.) Although this is a lower pressure than the cam Hertzian stresses, it is important to remember that in the equation for calculating EHD film thickness, the load is to the power 0.067. (See Table A-4.) At 300,000 psi (2,067 MPa) Hertzian stress, the formulation for thickness predicts an 8% decrease in film thickness compared to the 86,000 psi pressure measurements used in this work.

EHD Film – Forming Capability, h_o , microns

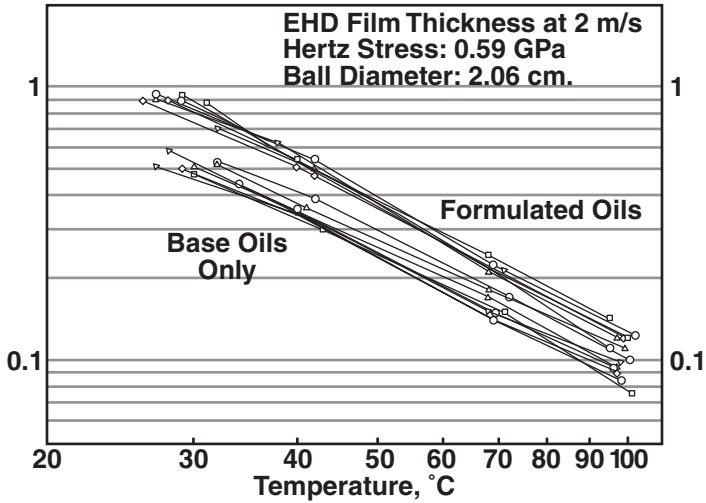


Figure 18 – EHD film forming capabilities versus temperature. Two different DI/VI formulations of API CG-4/SJ quality, using six different base stocks, ranging from API Group I to Group II.

EHD Film – Forming Capability, h_o , microns

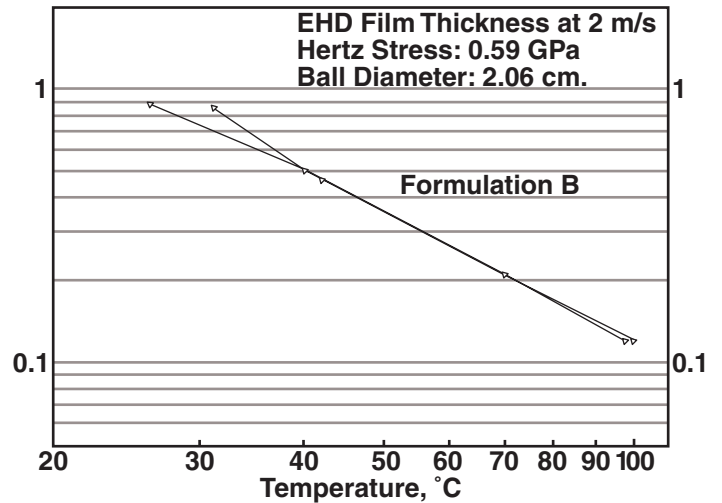


Figure 20 – EHD film forming capabilities versus temperature. One API CG-4/SJ oil using Group I (66% saturates) and Group II (99% saturates).

EHD Film – Forming Capability, h_o , microns

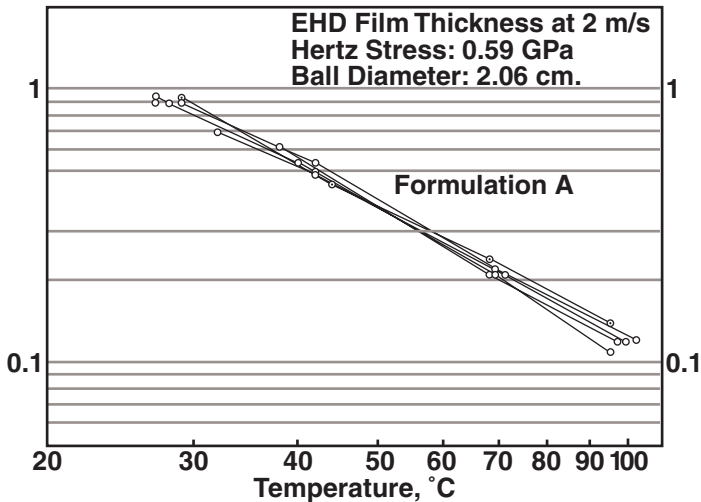


Figure 19 – EHD film forming capabilities versus temperature. One API CG-4/SJ oil using six different base stocks, ranging from API Group I to API Group II.

These findings are in close agreement with Lee and Patterson’s finding of 0.12 micron film thickness. Consequently to prevent asperity, contact surface finishes must be extremely smooth. These are often defined as super finished or microfinished camshafts.

ASPERITY CONTACT RESULTING IN CAM FAILURE

Elastic deformation of a roller is illustrated in Figure 21, showing the wear track of a roller on a cam lobe surface. Wear, in this case, is the result of asperity-asperity contact (i.e., metal-to-metal contact) that has produced “glazing” and contact fatigue micropitting.

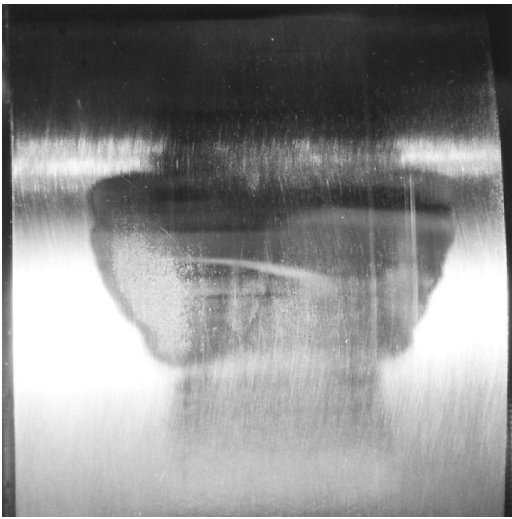
Evidently, the roller was crowned. On traversing the cam nose it elastically deformed, producing an image of the broader contact area of roller and cam lobe in the higher pressure cam nose area. Figure 22 shows a higher magnification view of an area exhibiting surface distress (glazing, followed by micropitting). Asperity-asperity contact (see Figure 23) at high pressures plastically deforms (i.e., flattens) the asperities. Areas of flattened asperities appear polished, but not smooth, hence the term “glazing.” Metal-to-metal contact implies the absence of lubricant. In concentrated contacts, metal-to-metal contact can be inferred from the lambda ratio:

$$\lambda = \text{Lambda Ratio} = \frac{\text{Lubricant Film Thickness}}{\text{Composite Surface Roughness}}$$

In this particular application, the measured surface roughness was 8 microinches and the EHD film thickness was estimated to be 4.8 microinches, hence $\lambda = 0.4$. As a rule of thumb, to prevent asperity contact $\lambda > 3$ is required. To increase λ to 3, a surface roughness of about 1.6 microinches would be required. To increase the lambda to 2, the average surface roughness needs to be 1.1 microinch.

At high Hertzian stress cam surface finishes must be smooth, however, smooth surface finishes will increase sliding. To prevent contact fatigue failures due to sliding, other independent variables must be correct. They are cam hardness, surface compressive stress, cam and roller geometry, and prompt, flooded lubrication.

Our experience indicates that “Thielenhaus” stone polishing provides a very consistent and smooth surface finish. A number of manufacturers have used this approach and significantly improved cam durability by reducing



Magnification 2.6x

Figure 21– Injector lobe showing glazing and micropitting, initiating steps (up-ramp)



Magnification 31x

Figure 22– Injector lobe showing glazing and micropitting, initiating steps (up-ramp)

surface finishes to 2 microinches R_a . However, the debris formed during the operation is not desirable, so some manufacturers use a paper polish finish.

Rpk surface finish measurement has provided a better direction to improving surface finish in cams. Alternatively, laser 3-D profilometer surface finish measurements are superior to stylus which is limited in scope. With these fine surface finishes, surface corrosion due to humidity after manufacture must be prevented by the use of grease or rust inhibitor lubricants to ensure surface integrity.

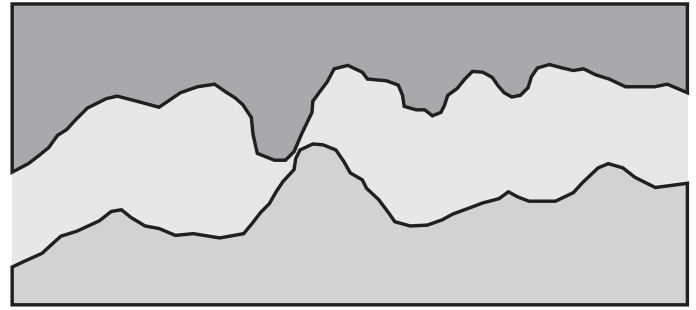


Figure 23 – Asperity-to-asperity contact.

The issue of increased sliding with smooth surface finishes remains an issue in some applications that are not well lubricated in cold starts or frequent stop-go operations. But the degree of lubrication at the surface can influence how smooth the surface finish should be to prevent failure.

A good example of the approach is the GM LT-1 V-8 gasoline engine cam. The new cam, according to our measurements, was 4.5 microinches R_a , that decreased to 3 microinches R_a after 4000 hours durability testing. It can be seen from the micrographs that the valleys, which provide the critical oil, can sustain 300,000-psi (2,067 MPa) Hertzian stress. In order for this finish to work successfully, the other nine parameters must also be correct.

This cam must be flooded with oil from both the crankshaft and the hydraulic lifters, due to its location in the V block. Consequently, the finish after running is glazed but without failures, as shown in Figures A-2 through A-3.

FLAT CAM PROFILE AND BARRELED ROLLER GEOMETRY

Elastic deformation of the roller at the high peak load has been illustrated in Figures 24 and 25. Consequently, in order to sustain these loads without failure, the roller needs an adequate crown and the cam must be flat.

If the cam face is bowed due to the hardening process, the end result is a point contact between the roller and the cam in which the Hertzian stress will exceed the capabilities of the cam.

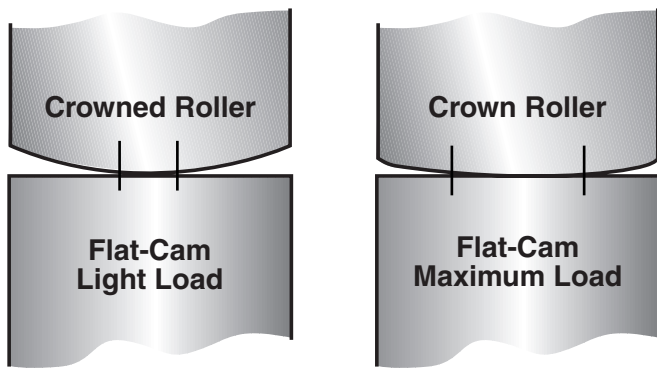


Figure 24 – Illustration of barrelled roller elastic deformation under load.

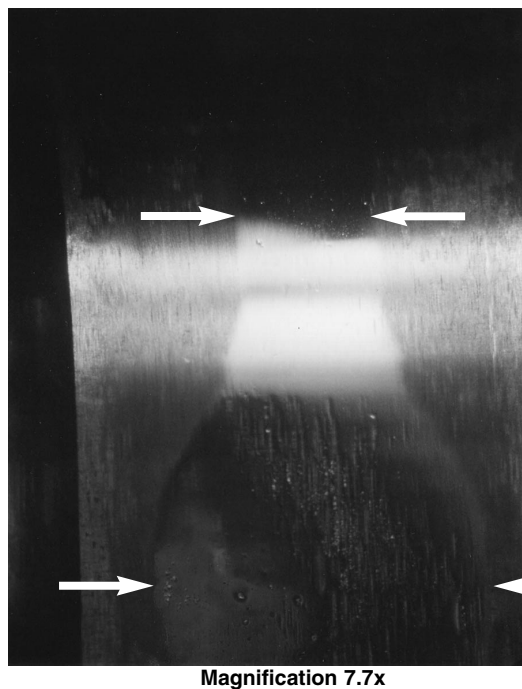


Figure 25 – Example of elastic deformation of roller shown on cam surface. Light load to maximum load.

Frequently induction hardened cams are only paper or stone polished as a final operation, as rapid grinding after hardening can anneal the surface. But if the bowing occurs in the order of 0.001-0.002 inch (0.0254-.0508 mm), contact fatigue may result. The cam lobe profile shown in Figure 26 had a bow of 24 μm (0.001 inch) and the cam failed. The cam lobe profile must be flat as shown in Figure 27. This may require slow grinding after heat treatment, if this is necessary to ensure flatness. It is critical that the cam lobe be flat but not concave, as this will cause edge loading by the roller.

In addition, the roller must be crowned. If the roller is flat it will cause edge-loading on the cam lobe at high loads and contact fatigue can occur.

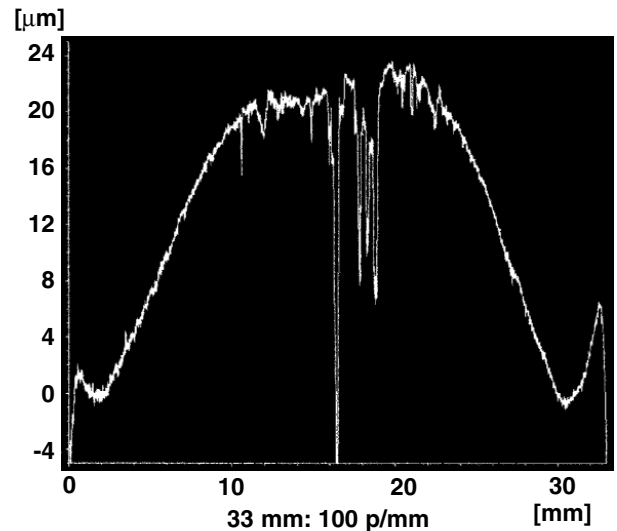


Figure 26 – Bowed cam lobe profile. Failed cam with contact fatigue from the field.

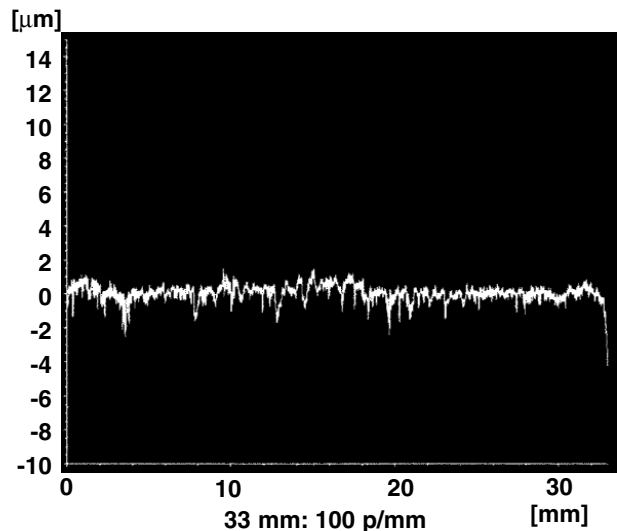


Figure 27 – Flat cam lobe profile. No failures at 500,000 miles (800,000 km).

CAM HARDNESS

To enable the above kind of surface finish to operate successfully, the cam must be extremely hard and homogeneous at the outer surface. In fact, the studies of Sui and Torng have shown that increasing cam hardness significantly improves cam roller reliability [4]. In our experience 60-64 Rc is the hardest surface finish achieved with either induction hardening or case hardening. Induction hardening provides the benefit of not having ovens for heating and is a relatively quick process.

In the case of the GM LT-1 cam that we benchmarked, we had conducted X-ray diffraction of the lobe, which indi-

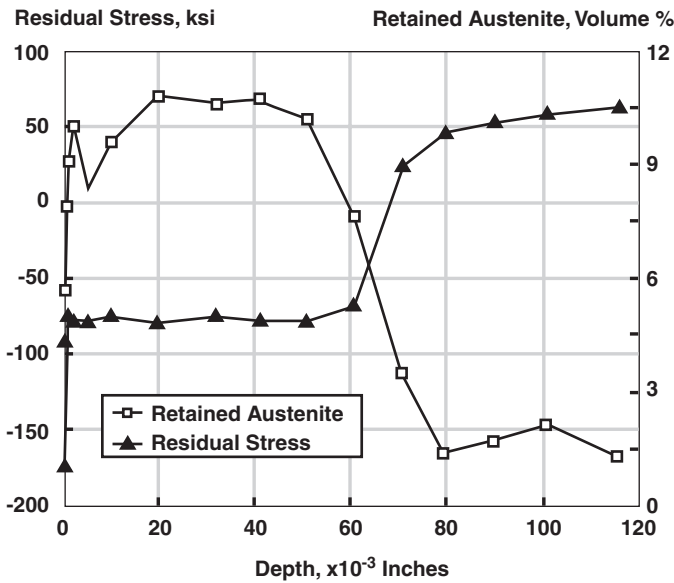


Figure 28 – GM-LT-1 cam lobe – x-ray diffraction analysis of compressive stress and retained austenite. Residual compressive stress – 175 ksi (–175,000 psi) at surface and 95% martensite structure.

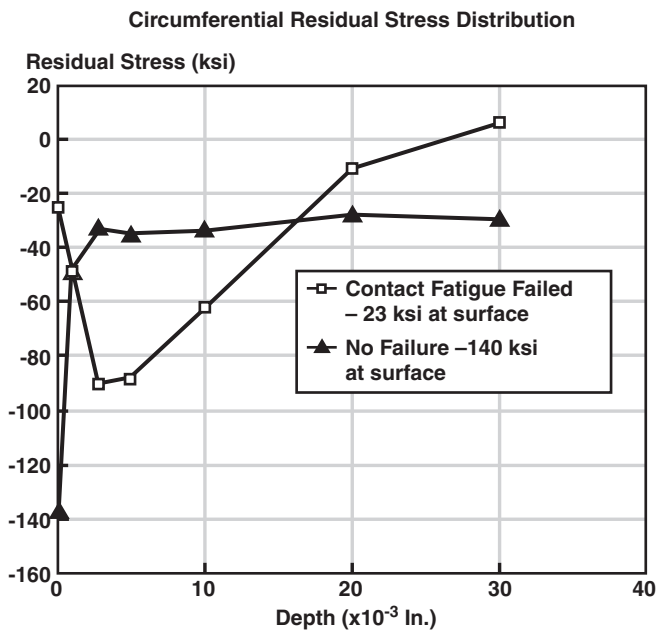


Figure 29 – X-ray diffraction analysis of one cam lobe with contact fatigue with compressive residue stress of – 23 ksi (– 23,000 psi) and second lobe with no failure with compressive stress at

cated 10% austenite, with the remaining 90% martensite to a depth of 0.05 inch; 95% martensite at a depth of 0.070 inch is the hardest structure that can be achieved.

We have examined a failed diesel camshaft in which the hardness varied between adjacent lobes. One injector lobe failed with contact fatigue with a hardness of 47-48 Rc, while the adjacent lobe was harder at 54-57 Rc, and had no sign of failure. These two lobes also varied considerably in regard to surface compressive stress.

RESIDUAL SURFACE COMPRESSIVE STRESS

Increasing surface hardness and compressive residual stresses also significantly improves cam reliability [4]. The benchmarked LT-1 cam had a residual compressive stress of –175 ksi. (See Figure 28.)

In contrast, the above-mentioned failed diesel camshaft had varied hardness between the lobes and varied compressive stress. In this application one lobe failed by contact fatigue while the next lobe was in perfect condition. In conducting X-ray analysis on both these lobes, we found that the failed lobe had a compressive stress of only –23 ksi (hardness 47 Rc). In contrast, the lobe in satisfactory condition had a higher compressive stress of –140 ksi (hardness 50 Rc). (See Figure 29.)

CONTACT FATIGUE FAILURE OF THE INJECTOR LOBE

Contact fatigue failure can result from a combination of the individual parameters reviewed above, or from just one of these parameters not being correct. This is particularly the case in applications where the engine is frequently shut down and restarted, which can result in both a lack of lubrication and roller skidding.

In our experience with one engine with 80,000 miles (129,000 km) of service, cam contact fatigue failure of the injector lobe first occurred at the cam roller interface, approximately 10-15 degrees before the nose of the cam. (See Figure 30.) All the bronze pins in this application were in perfect condition. This initial failing point progressed to cause damage to the cam nose and down the ramp. (See Figures 31 and 32.) It is important to

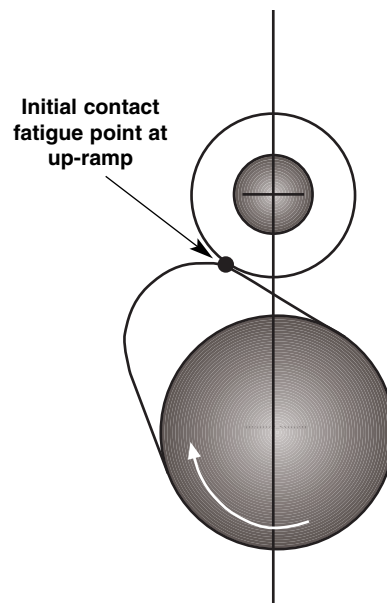
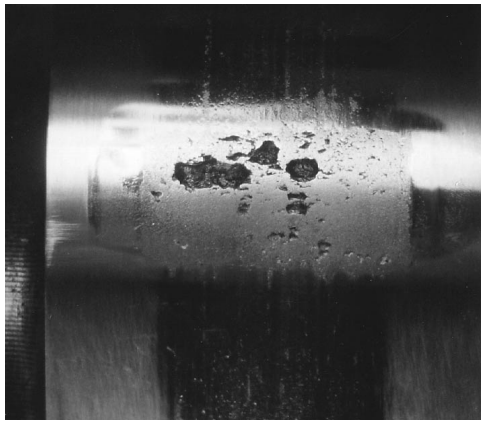
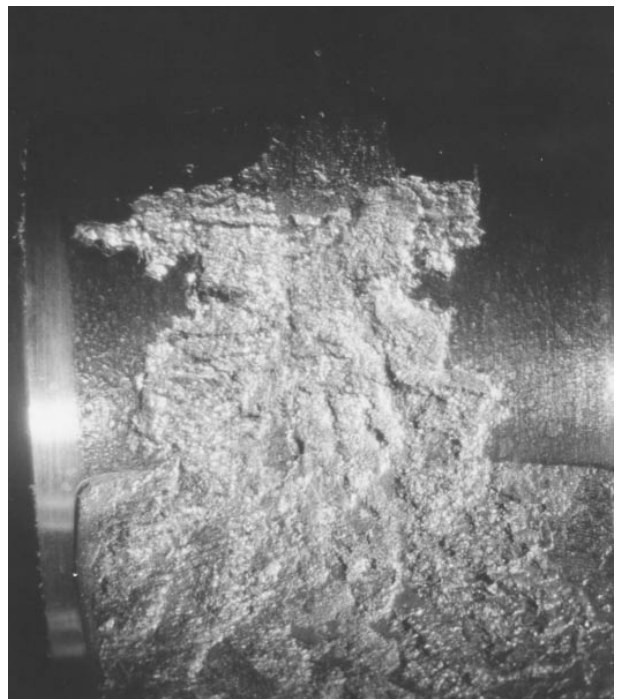


Figure 30 – Contact fatigue first before cam nose – then damage occurs on down-side of cam.



Magnification 2.6x

Figure 31 – Injector lobe – fatigue pitting in advanced stage (up-ramp)



Magnification 2.6x

Figure 34 – Injector lobe, showing pitting, denting, and spalling.

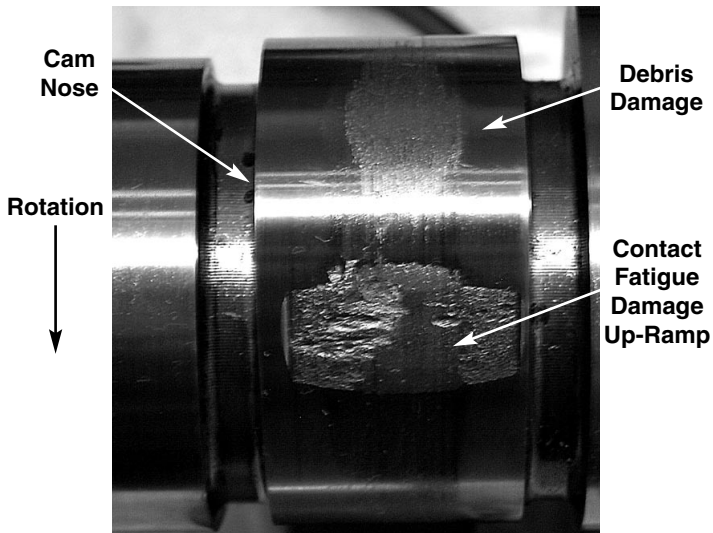
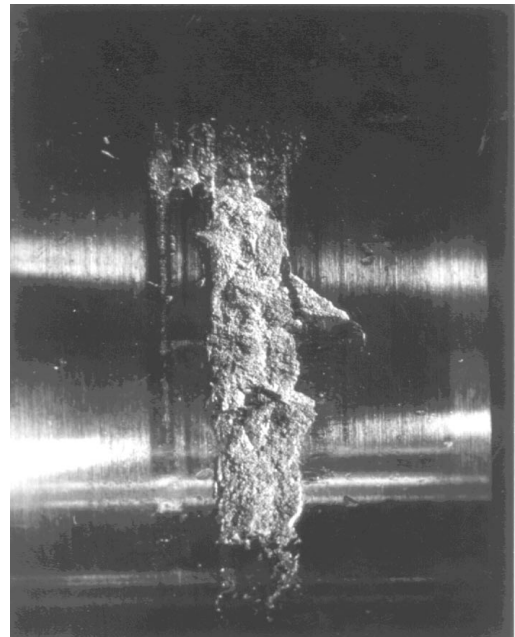
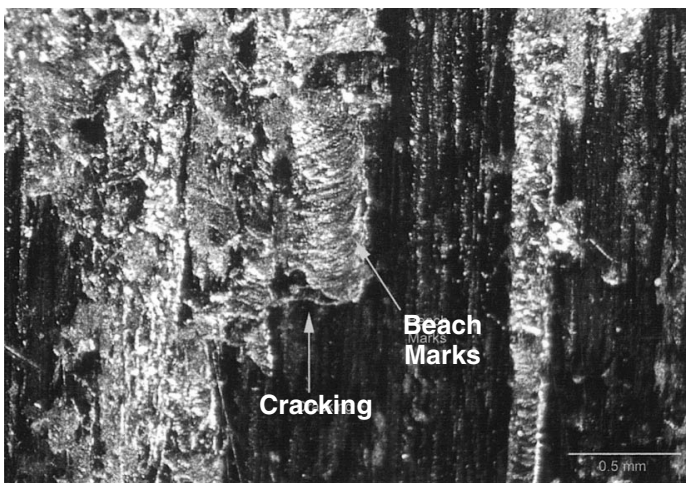


Figure 32 – Contact fatigue on up-ramp with subsequent damage on nose and down ramp.



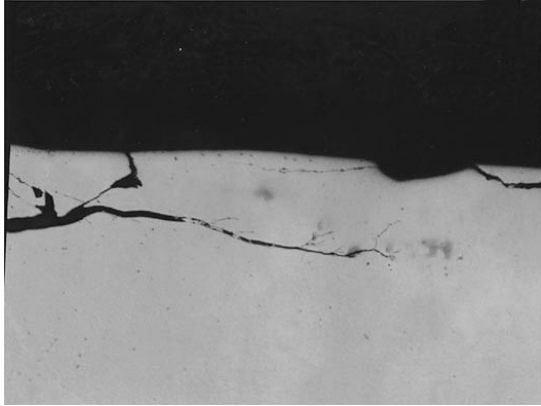
Magnification 2.6x

Figure 36 – Injector lobe showing spalling, cracking and denting.



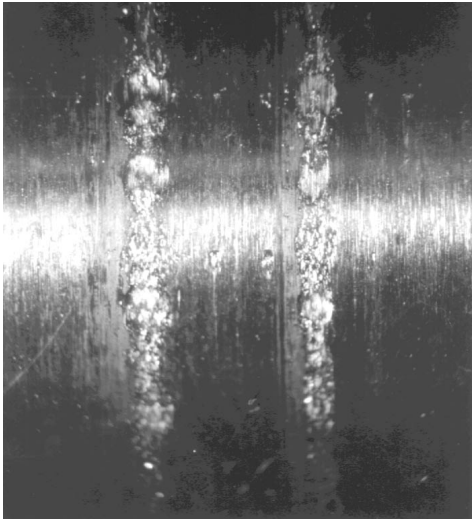
Magnification 25x

Figure 33 – Injector lobe at nose of cam (500,000 miles, 800,000 km) contact fatigue.



Magnification 250x

Figure 35 – Cross-section of metallographic section of failed cam lobe.



Magnification 2.6x

Figure 37 – Injector lobe showing pitting, “skidding”, adhesive wear and denting.



Magnification 10x

Figure 38 – Injector roller – pitting, sliding wear, and denting.

define the initial failure point in order to take corrective action, as subsequent damage often makes the failure hard to define.

These injector lobe failures were initiated by contact fatigue, leading to cracking and subsequent benchmarks as shown in Figure 33. In more advanced stages, the contact fatigue is clear, as shown in Figure 34-36. The subsurface cracking is apparent in some cases. (See Figure 35.) In other cases, skidding, or adhesive and denting damage due to passage of wear debris from other failing cams are evident. (See Figure 37 and 38.)

These failures occur relatively early in the engine life when one or a combination of the 10 factors affecting fatigue are not correct. In our experience, by 200,000 miles the contact fatigue is clearly evident, with the initial failure occurring by 80,000 miles (129,000 km). It is interesting that these failures are not predicted by used oil analysis.

FAILURES OF THE INTAKE AND EXHAUST LOBES

Injector lobe failures often resulted in subsequent failures of the injector, intake, or exhaust lobes. This is because debris from the injector lobe failure may cause abrasive wear of the roller pins or adhesive wear due to debris lodged between the contact surfaces, resulting in roller-cam lobe sliding.

Examples of intake lobe failures due to contact fatigue and roller skidding are shown in Figure 39 and 40.



Magnification 23x

Figure 39 – Intake lobe failure showing bench marks, contact fatigue and leading edge of damage area.



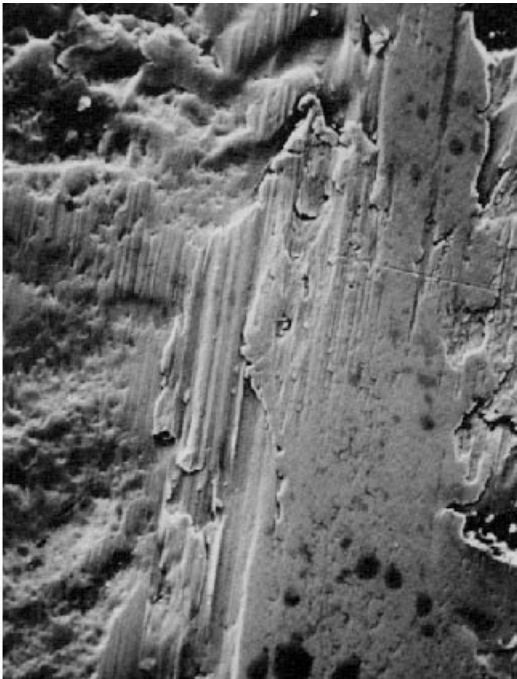
Magnification 31x

Figure 40 – Intake rollers having sliding damage with plastic flow and contact fatigue pitting.



Magnification 300x

Figure 42 – Exhaust valve cam lobe surface showing contact fatigue.



Magnification 300x

Figure 41 – Exhaust valve cam lobe surface showing abrasion, adhesion and contact fatigue.

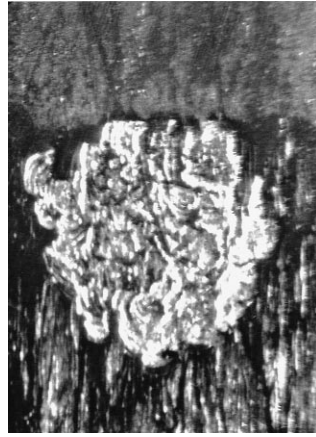


Magnification 40x

Figure 43 – Exhaust lobe – contact fatigue.



Magnification 30x



Magnification 60x

Figure 44 – Roller follower with bronze pin showing “skidding” and contact fatigue on steel roller.

Similarly, the exhaust lobes have shown contact fatigue and abrasion and adhesion due to wear debris passing through the contact. (See Figures 41-43.) Roller follower skidding and contact fatigue is shown in Fig. 44.

In some cases the exhaust or intake valve will fail independently from the injector. This can be due to the different contour used in these intake and exhaust lobes, which may have rapid accelerations and cause skidding. In addition, these lobes often do not have an adequate surface finish.

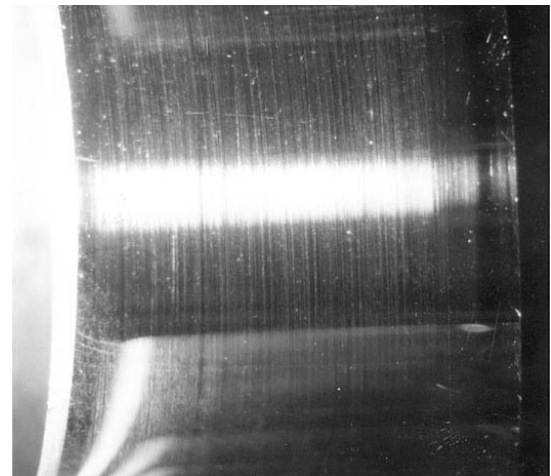
Frequently, the injector lobes are stone polished, but the valve lobes are only ground, to reduce costs. It is key to microfinish all the lobes to a smooth finish by Thielenhaus stone polishing or paper polishing, in order to prevent asperity contact. Improving the surface finish as measured by Rpk has eliminated lobe cam failures.

LOW FRICTION BETWEEN THE CENTER BRONZE PIN AND ROLLER

Low friction between the central pin and the roller is essential for minimizing wear, and skidding of the roller. However, contact fatigue debris from the lobes may cause secondary damage to the pin-roller interface, resulting in bronze pin wear and sliding of the roller on the cam surface. Alternatively, inadequate lubrication during frequent starts will result in bronze pin wear. A disadvantage of the bronze pin is its relative softness, which makes it readily abraded. Examples of this damage show abrasive wear of the pin and the inside of the roller. (See Figures 45-46.) Alternatively, due to high friction, the oil to the pin has become extremely hot and pyrolyzed. In some cases due to the high friction, the pin had rotated from its fixed position and cut off its oil supply hole. (See Figures 47 and 48.)



Figure 45 – Exhaust roller bronze pin showing wearstep.



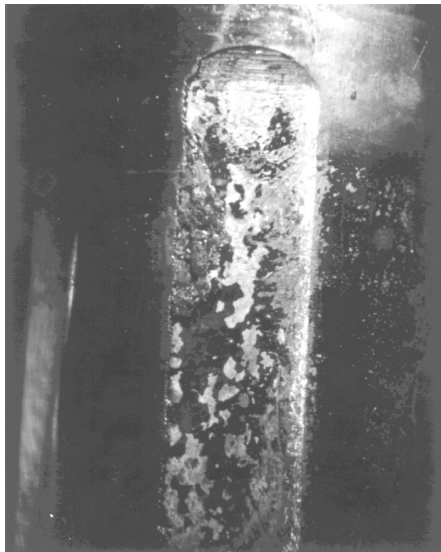
Magnification 5x

Figure 46 – Inside surface of steel using bronze pin roller,



Magnification 5.1x

Figure 47 – Injector bronze pin showing abrasive, erosive and adhesive wear.



Magnification 2.6x

Figure 48 – Injector bronze pin – deposit on the flat due to pyrolyzed lubricating oil due to excessive heating.

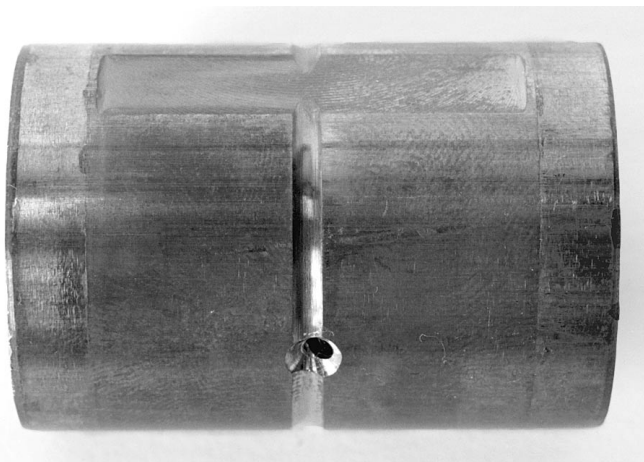


Figure 49 – Improved lubrication of a large diameter bronze pin through the use of an oil distribution groove around the periphery of the pin.

The bronze pin design is pivotal to preventing cam lobe contact fatigue failures. Consequently engine manufacturers have made significant improvements in its design. They include:

- Improving lubrication through prompt oil delivery, changes to the clearance between the pin and roller to retain oil on engine start-up, and in some cases the incorporation an oil groove in the pin. (See figure 49)
- Increasing hardness through proprietary techniques.
- Ensuring cleanness of the joint between the pin and roller.
- Reducing stress by increasing the pin's diameter.

These improvements, combined with changes in the other parameters previously discussed, have enabled engine manufacturers to successfully improve cam life using the bronze pin.

CERAMIC ROLLER AND STEEL PIN PROVIDES LOW FRICTION AND LOW WEAR UNDER MARGINAL LUBRICATION CONDITIONS

In stop-go vehicles or vehicles that have frequent shut downs to save fuel, the low friction between the center pin and roller is critical. We have found numerous failures of bronze pin-roller combinations, yet we have found none with the use of the silicon nitride roller and steel pin, provided the Hertzian stress is within the capability of the ceramic roller, and the ceramic porosity is correct and controlled. (See Figures 50 and 51.)

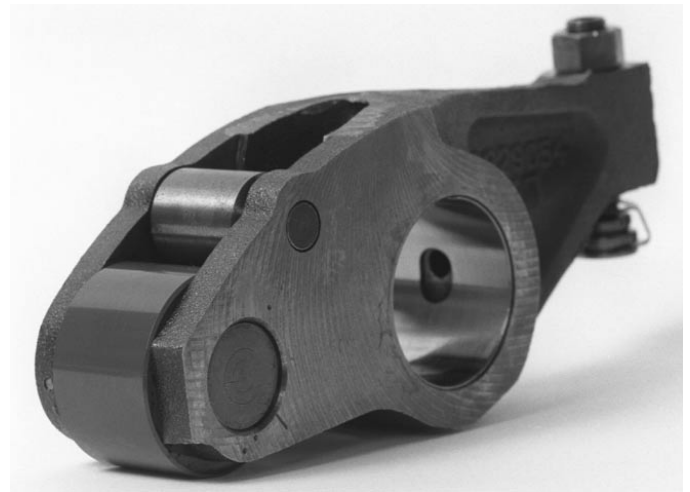


Figure 50 – Rocker arm configuration – injector silicon nitride roller and steel pin.



Figure 51 – Silicon nitride roller and steel pin after 4,000 hours durability testing.

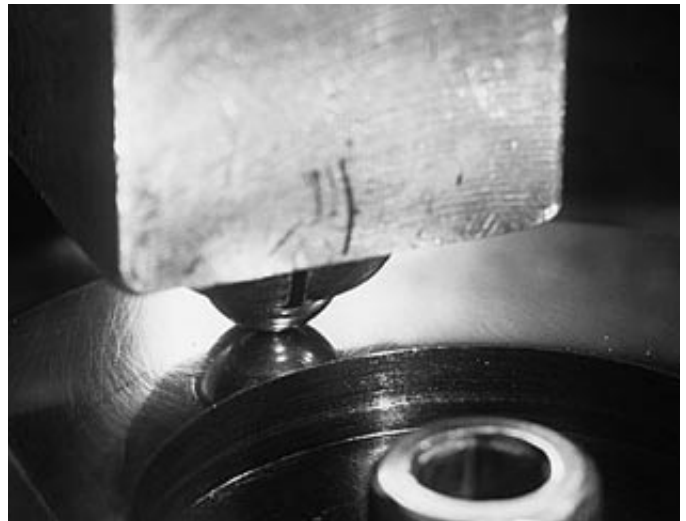
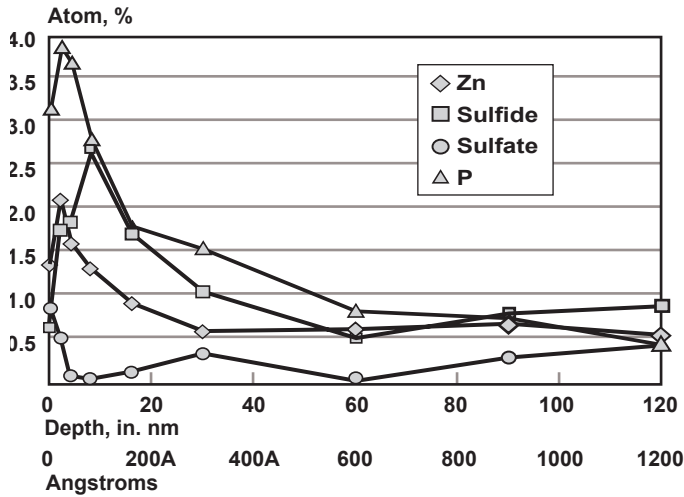


Figure 53 – Ball on flat tribometer contact.

Figure 52 – ESCA depth profile on steel axle used in ceramic roller follower. Zinc, phosphorus and sulfur adsorber on to axle, providing a protective wear film.

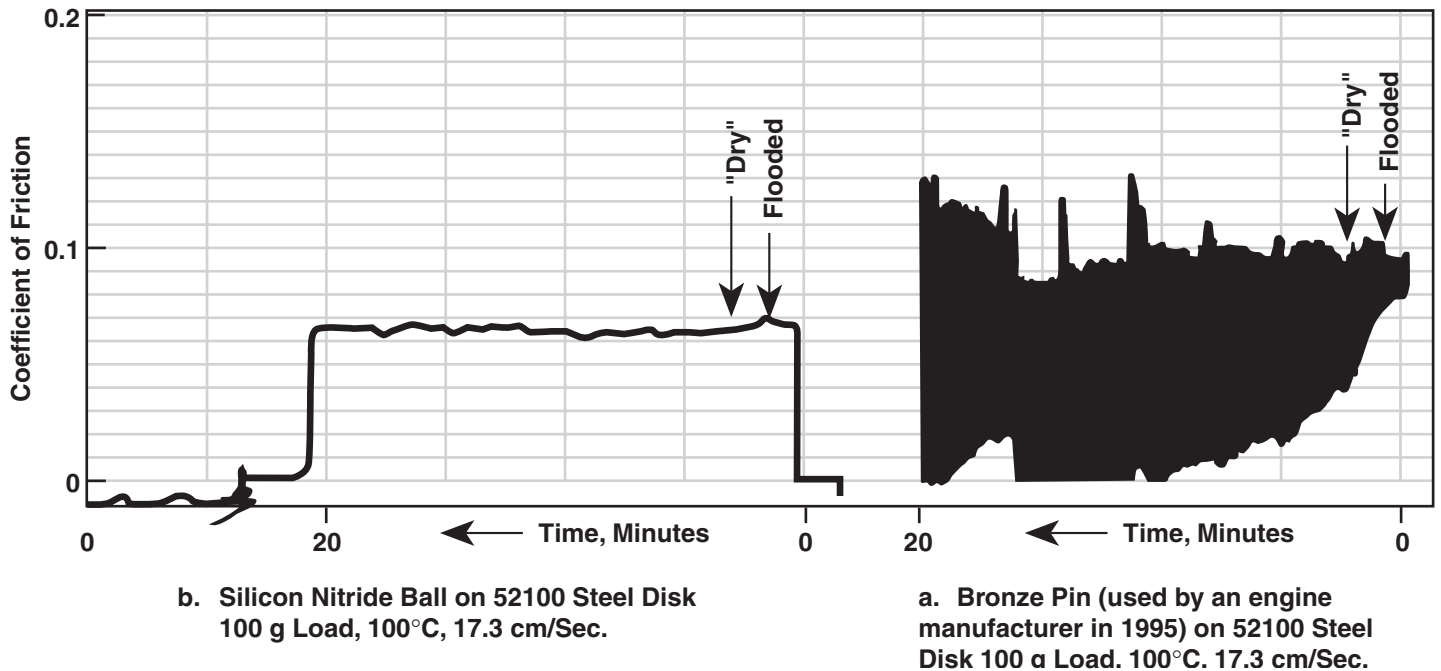


Figure 54 – Friction versus time alternately flooded with API CG-4/SJ – SAE 15W-40 oil (~2 min.) and “dry” (~1 min.).
 a. Range of motion of the recorder pen in measuring friction. The silicon nitride ball had low and constant friction under flooded and starved conditions. In contrast, the bronze pin had severe stick-slip with very high friction under starved conditions; and high friction with stick-slip under flooded conditions that would cause roller skidding on the cam.

In addition, because there are no failures of the injector lobe, there is no secondary damage to the other lobes.

The silicon nitride roller has a number of advantages.

- Its Inertia is One-Third That of Steel, Which Allows Quick Accelerations
- It Has Excellent Compatibility With Steel
- It Has an Extremely Smooth Surface Finish (Measured at Ra 1.6 Microinch/0.04 μm)
- It is Extremely Hard (Measured at 75 Rc)

In addition, the ZnDTP wear inhibitor readily forms an anti-wear film on steel and not on bronze. Through the use of ESCA analysis, we demonstrated a ZnDTP antiwear film through the presence of sulfur, phosphorous, and zinc on a steel pin from an engine test. (See Figure 52.)

To demonstrate its advantage over the bronze pin in stop-go applications, we used a silicon nitride ball and a bronze pin- (hemispherical end) on-flat tribometer. (See Figure 53.)

Table 1

Sliding Conditions, Ball-On-Flat Tribometer Experiments

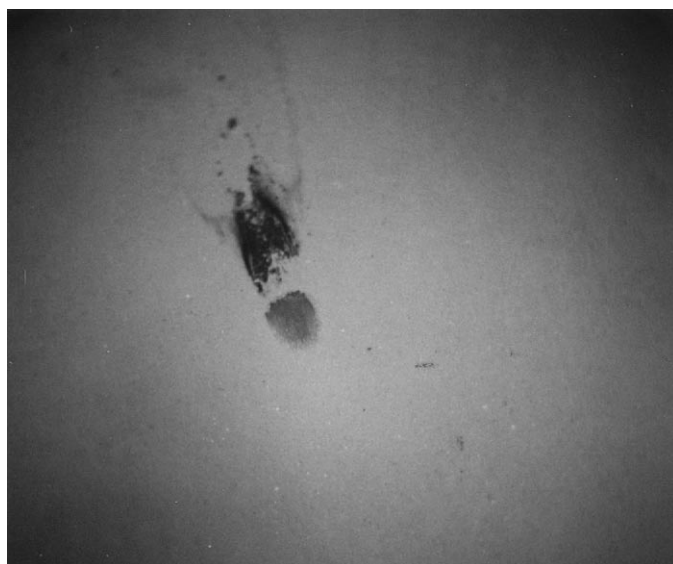
Load, N	4.90
Initial Contact Pressure, N/m ²	7.1 x 10 ⁸ (1.04 x 10 ⁵ psi)
Initial Contact Area, cm ²	6.9 x 10 ⁻⁵
Sliding Speed, cm/Sec.	17.3
Temperature, °C	100
Run Time, Sec.	3600
Atmosphere	Laboratory Air
10-Min. Break-in, speed, cm/Sec.	17.3

	Sliders	Flat
Material Hardness	0.635 cm Diameter Silicon Nitride Ball	52100 Steel R _C ~58
Surface Roughness	0.635 cm Diameter Bronze Pin With Hemispherical End	R _a =0.051 μm

The silicon nitride ball had low and constant friction under flooded and starved conditions. In contrast, the bronze pin had severe stick-slip with very high friction under starved conditions; and high friction with stick-slip under flooded conditions that would cause roller skidding on the cam. (See Figure 54.) The silicon nitride wear scar was minimal compared to bronze. (See Figures 55 and 56.) Other researchers have demonstrated the benefits of ceramics in valve-train systems or fuel pump applications [21-24]. This silicon nitride steel pin configuration is significantly more expensive than the bronze pin.

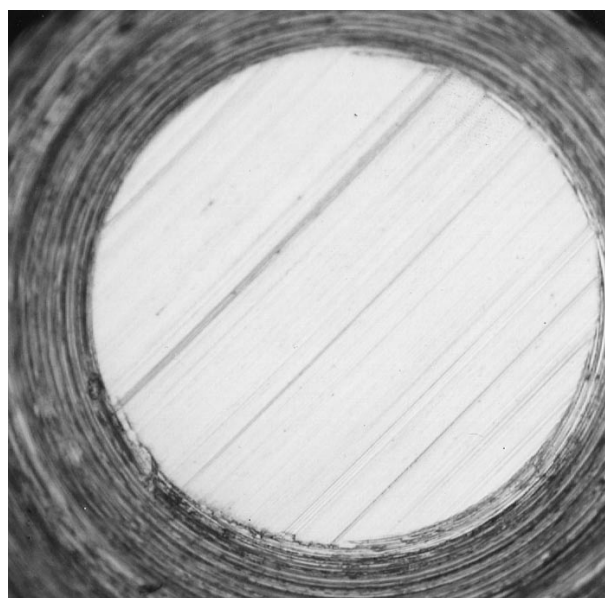
Our experience with fleet maintenance managers indicates that due to the characteristics reviewed above, the silicon nitride roller has been very successful in line haul operations and in stop-go application with frequent engine shut downs.

Nevertheless, Hertzian stress and the porosity of the ceramic must be closely controlled. In one instance where it exceeded these requirements, failures did occur until the stress was reduced. (See Figure 57.)



Magnification 103x

Figure 55 – Silicon nitride ball (Norton), wear scar from the tribometer wear test.



Magnification 103x

Figure 56 – Bronze pin wear scar from the tribometer wear test. Bronze pin cut from engine roller follower pin.



Figure 57 – Experimental ceramic roller operating at too high an Hertzian stress.

STAYING WITHIN THE STRESS CAPABILITY OF THE CAM AND ROLLER

In all cases, the roller and cam must stay within the stress capabilities of the material. If cam profiles are such that the stress increases beyond the capabilities of the material, contact fatigue will occur.

ALIGNMENT OF ROLLER ON THE CAM

Skewing of the roller on the cam has two detrimental effects. First, it will cause wear and contact fatigue. And secondly, as pointed out by Bair and Winer [6], it increases sliding, which is detrimental in regard to increasing Hertzian stress. We have seen this type of failure in both the injector lobe and intake or exhaust valves. Crack formation is the contact fatigue failure. (See Figures 58 and 59.)

PROPER VALVE CLEARANCE SETTINGS

The Hertzian stress on any of the lobes is affected by incorrect valve clearances. If valve clearances are too wide the roller will not be on the cam ramp and the Hertzian stress will increase and result in subsequent failure. Although this is rare, in our experience it is still a potential contributing factor.

DISCUSSION

Engine manufacturers have made major advantages in developing durable cams for low emission engines. However, trying to reduce costs of critical components

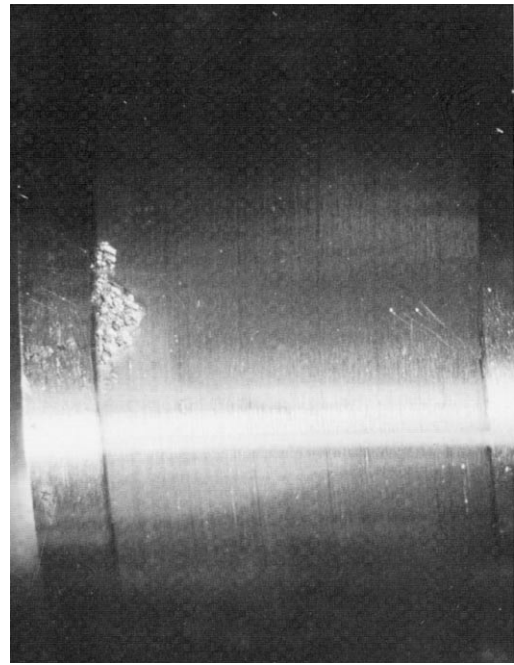


Figure 58 – Intake cam lobe showing contact fatigue pitting due to misalignment.

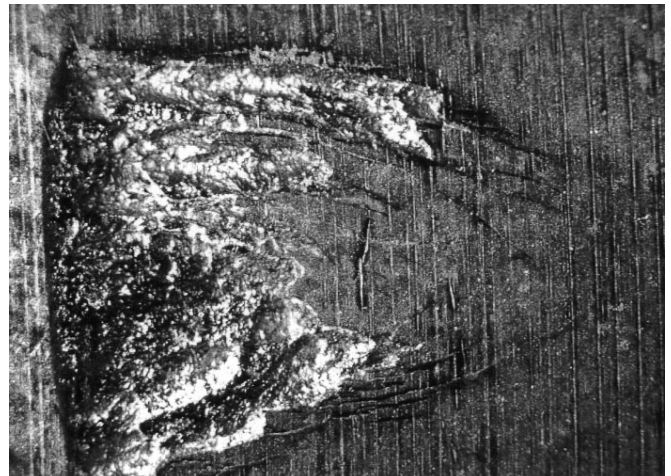


Figure 59 – Side of cam lobe showing contact fatigue near nose due to misalignment.

such as cams, where surface finish, hardness, geometry and lubrication are critically important, can be a major error. In regard to both the camshaft and the crankshaft, there should be no compromise of quality in these characteristics.

As injection pressures continue to increase, the common-rail fuel system, which is pressurized by a separate pump and timing controlled electronically, may become more advantageous, as it eliminates the cam from pressurizing the fuel injectors. These systems are successfully used in 300 to 3000 bhp engines. However, the type of systems selected in the future will be determined by which one meets the proposed emission standards for 2007 shown in Figure 1.

CONCLUSIONS

With the drive to reduce emissions and improve fuel economy in the 1990s, camshaft lobe contact fatigue became the "Achilles heel" of low emission engines of several engine types.

Our experience in cam failure analysis indicated that rolling contact fatigue was the major failure mechanism. In order to prevent these failures there are 10 independent variables which must be controlled:

1. Prompt and Adequate Lubrication to the Central Roller Pin and Cam-Roller Surfaces.
2. Use of Oil Formulations Meeting API CG-4 or CH-4 Requirements
3. Staying Within the Stress Capability of the Cam and Roller
4. Low Friction Between the Roller Pin and Roller
5. Surface Finishes That Minimize Asperity Contact
6. Extremely Hard Cam Lobe and Roller Surfaces
7. Residual Surface Compressive Stresses
8. Flat Cam Lobe Surface and Crown Roller Geometry
9. Proper Injector and Valve Clearance to Minimize Stress, and
10. Correct Alignment of Cam Lobe and Roller

Because sliding of the roller on the cam moves the area of maximum stress towards the surface, each of the parameter reviewed above must be correct to prevent failures, particularly in vehicles with frequent engine shut downs and starts, and stop-go service.

In this regard, in bench tests simulating stop-go applications, we found that the silicon nitride roller on a steel pin had low and constant friction under flooded and starved lubrication conditions. In contrast, the bronze pin and steel roller had severe stick-slip with very high friction, which could cause roller skidding on the cam. The silicon nitride roller and steel pin has provided long cam life, across many engine applications.

Low friction between the roller pin and the roller is pivotal to preventing cam failures. Consequently, engine manufacturer's using the bronze pin have changed its design by: improving the pin's lubrication, increasing the pin's hardness, reducing the pin's stress and ensuring cleanliness of the pin's joint. These improvements have significantly improved cam life.

ACKNOWLEDGMENTS

The authors would like to thank Chevron Products Company for permission to publish this paper and express their special appreciation to:

Jim Ziemer and Allan Beckman, the current tribologists at Chevron, for helping provide analysis of cam failures and for reviewing this paper.

Fleet-maintenance managers who provided failed cams for analysis.

Anil Kulkarni of GM, for his guidance and advice on this topic and for providing a GM LT-1 for analysis.

And finally, to all those who reviewed this paper for their valuable comments and suggestions.

REFERENCES

1. Caterpillar Tractor Company, Wall Street Journal, November 22, 1999.
2. D. C. Sun and R. C. Rosenberg, "An Experimental Study of Automotive Cam-Lifter Interface Friction," ASLE Transactions, Vol. 30, pp 167-176 (1986).
3. J. Lee and D. J. Patterson, "Analysis of Cam-Roller Follower and Slippage in Valve Train System," SAE 951039 (1995).
4. P. C. Sui and T. Torng, "Cam-Roller Component Fatigue Reliability Analysis," SAE 950708 (1995).
5. P. E. Duffy, "An Experimental Investigation of Sliding at Cam to Roller Tappet Contacts," SAE 930691 (1993).
6. S. Bair and W. O. Winer, "A Technique for Measuring Roller Follower Skidding on Automotive Camshafts," Proceedings of the 17th Leeds-Lyon Symposium of Tribology, September 4-7, 1990, Paper 6. Tribology Series 18, Elsevier (1991).
7. J. C. Wall, "Impact of U.S. Emission Regulations on Heavy-Duty Diesel Engine Development in 1990's," Congress International, Moteurs Diesel: Perspectives 1990-2000, Society des Ingenieurs de L'Automobile, Lyon, France, June 12-13, 1990.
8. J. A. Mc Geehan and K L Eiden, "Low Temperature Pumpability in Emission Controlled Diesel Engine," SAE 2000-01-1989, (2000).
9. J. A. Mc Geehan et al, "The World's First Diesel Engine Oil Category for Use With Low Sulfur Fuel: API CG-4," SAE 941939 (1994).

10. J. A. Mc Geehan et al, "New Diesel Engine Oil Category for 1998: API CH-4," SAE 981371 (1998).
11. P. R. Ryason, I. Y. Chan, and J. T. Gilmore, "Polishing Wear by Soot," Wear, 137 pp 15-24 (1990).
12. C. Kim, C. Passut, and D. Zang, "Relationships Among Oil Composition Combustion-Generated Soot and Diesel Engine Valve Train Wear," SAE 922199 (1992).
13. E. Bardasz, V. A. Carrick, H. F. George, M. M. Graf, R. E. Kornbrekke, and S. Pocinki, "Understanding Soot Mediated Oil Thickening Through Design Experimentation – Part 5: Knowledge Enhancement in the GM 6.5L," SAE 9729752 (1997).
14. D. Dowson and G. R. Higginson, "Elastro-Hydrodynamic Lubrication – The Fundamentals of Roller Gear Lubrication," Pergamon Press (1966).
15. R. D. Hercamp, "Reducing Durability Due to Friction Modifier in Heavy Duty Diesel Lubricants," SAE 851260 (1985).
16. J. A. Mc Geehan, E. S. Yamaguchi, and J. Q. Adams, "Some Effects of Zinc Dithiophosphates and Detergents on Controlling Engine Wear," SAE 852133 (1985).
17. J. A. Mc Geehan and P. R. Ryason, "Million Mile Bearings: Lessons From Diesel Engine Bearing Failure Analysis," SAE 1990-01-3576.
18. E. Hoglund, "Subsurface Stresses in Lubricated Rolling-Sliding Elastohydrodynamic Line Contact Considering Limited Shear Strength of the Lubricant," Proceedings of the 12th Leeds-Lyons Symposium on Tribology, September 3-6, 1985, Butterworths.
19. Y. F. J. Westlake and A. Cameron, "A Study of Ultra-Thin Lubricant Films Using an Optical Technique," Symp. Experimental Methods in Tribology Proc., I. Mech. E. 182, Pt 3G pp 75-80 (1967-1968).
20. L. D. Wedeven, J. A. Mc Geehan, and P. R. Ryason, "Diesel Engine Oils Formulated With Hydrocracked and Solvent Refined Base Stocks Have Equal EHD Film Thickness," Tribology Transactions, Vol. 40 (1997), 3, 453-460.
21. A. Gangopadhyay, H. S. Cheng, S. T. Harman, and J. M. Corwin, "Evaluation of Tribological Performance of Ceramic Roller Follower," SAE 900401 (1990).
22. R. Southam, J. Reinicke-Muramann, P. Krieter, and G. Roger, "Analysis of Potential Improvements in Engine Behavior Due to Ceramic Valve Train Components," SAE 900452 (1990).
23. K. Noda, S. Kamiya, T. Fujimura, and K. Taniguchi, "Development of Ceramic Roller for Diesel Distributor-Type Fuel Injection Pump." JSAE Review 20, pp 197-201. (1999).
24. G. Bartelt, R. Becker, and B. Zimmermann, "Extreme-Pressure Behavior of Lubricated Ceramic-Steel Couples," Lubrication Science, Vol. 10, pp 27-42, November 1997.
25. Dowson, D. and Higginson, G.R., "Proc. Inst. Mech. Engr., Vol 182, Part 3A, pp 151-167, 1968.
26. Hamrock, B.J. and Dowson, D. "Isothermal Elastohydrodynamic Lubrication of Point Contact - Part III - Fully Flooded Results," ASME J. Lubr. Tech., Vol. 99. pp 264-276, 1977.

TABLE A-1

Ball	13/16-In. Diameter M-50 (Grade 5)
Disc	4-In. Diameter x 0.5-Inch Thick, Pyrex 7740 With Optical Coating
Max. Hertz Stress	0.59 GPa (86,000 psi)
Rolling Velocity	Variable
Temperatures (Nominal)	23°C (Ambient), 40°C, 70°C, and 100°C

TABLE A-2

API Base Stock Categories

Group	Sulfur, Wt %		Saturates	V.I.
I	>0.03	and/or	<90	80-119
II	≤0.03	and	≥90	80-119
III	≤0.03	and	≥90	≥120
IV	All Polyalphaolefins (PAOs)			
V	All stocks not included in Groups I-IV (Pale oils and non-PAO Synthetics)			

TABLE A-3

Base Stocks Used in EHD Film Thickness Measurements

Saturates	Group I	Group II	Oil Supplier
66%	✓		1
67%	✓		2
73%	✓		3
73%	✓		4
77%	✓		5
99%		✓	6

Average Roller Axle Wear, x10⁻³ Inches

μm 12.7

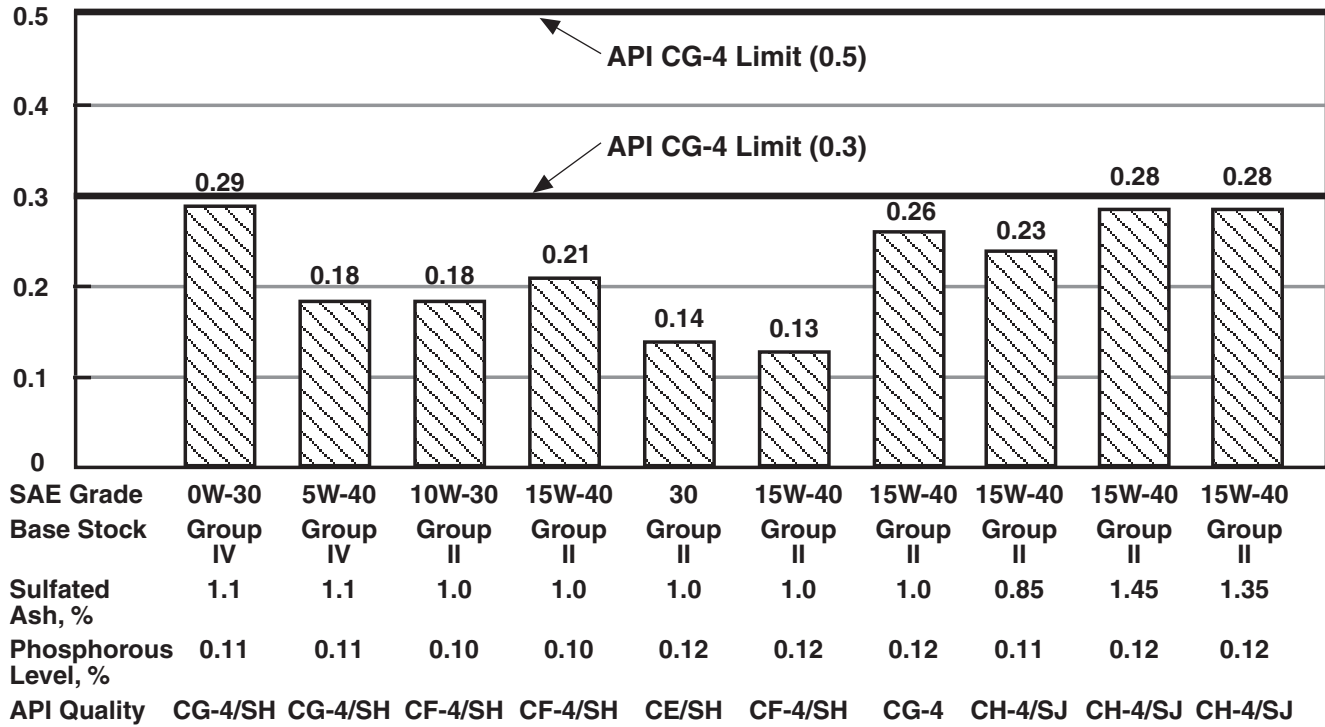


Figure A-1 – GM 6.2 liter roller follower wear test (5% soot)



Figure A-2 – Engine cam showing surface glazing in V-8 engine surface fully flooded in oil.



Figure A-3 – Engine cam showing surface glazing in V-8 engine. Surface is fully flooded with oil.

TABLE A-4
EHD film Thickness Predictions

Recall that the formula for the EHD film thickness is:

$$h_o = 1.9 \frac{(\eta_o U_e)^{0.67} \alpha^{0.53} R^{0.397}}{E' 0.073 W^{0.067}}$$

where:

- h_o = The central film thickness.
- R = The combined radius of curvature.
- η_o = The viscosity at ambient temperature and pressure.
- U_e = The entraining velocity (average) of the surface velocities of the ball and disk.
- E' = The combined elastic modulus.
- w = The load.

The low pressure low shear viscosity η_o is the viscosity routinely measured by capillary viscometry. Hence, the larger η_o is, the larger the EHD film thickness will be.

For line contact the film thickness is:

$$H_{\min} = 2.65U^{0.7} G^{0.54} W^{-0.13}$$

The central film thickness for line contact can be derived from the relation (2)

$$H_c/H_{\min} = 1.15 U^{-0.007} G^{0.02} W^{0.03}$$

For point contact the film thickness

$$H_{\min} = 3.63U^{0.68} G^{0.49} W^{-0.073} (1-e^{-0.68K})$$

$$H_c = 2.69U^{0.67} G^{0.53} W^{-0.067} (1-e^{-0.73K})$$

where,

$$k = a/b$$

a = 1/2 the contact width in the perpendicular to the rolling direction

b = 1/2 the contact width in the direction of rolling for contact point, $k = 1$

COMMONLY USES EHD FILM THICKNESS EQUATIONS (Ref. 25 and 26)

Calculation of EHD film thickness is accomplished by commonly used film thickness equations for line contact (1) and point, or elliptical, contact (2). These equations are formulated with dimensionless parameters.

$$H_{m,c} \text{ dimensionless film thickness} = h_{m,c}/R$$

$$U \text{ dimensionless speed parameter} = (\mu_o u)/(E R)$$

$$G \text{ dimensionless materials parameter} = \alpha E$$

$$W \text{ dimensionless load parameter} = w/(E R)$$

where,

h_m = film thickness at the rear constriction

h_c = film thickness at center of contact

μ_o = viscosity at atmospheric pressure

α = pressure-viscosity coefficient

u = velocity defined as $u = 1/2 (u_1 + u_2)$ where u_1 and u_2 are the individual velocities of the moving surfaces

R = radius of equivalent cylinder

w = load per unit width for line contact, or total load for point contact

E = elastic modulus of equivalent cylinder
 $1/E = 1/2 ((1-\sigma_1^2)/E_1^2 + (1-\sigma_2^2)/E_2^2)$

E_1, E_2 = elastic modulus for bodies 1 and 2

$\sigma_{1,2}$ = poisson's ratio for bodies 1 and 2